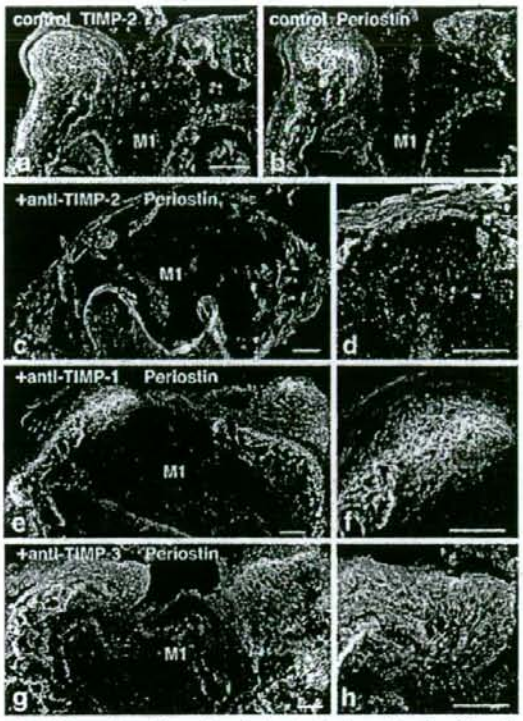

Fig. 8 Loss of staining of periostin in gingiva cultured with anti-TIMP-2 antibody (*M1* molar). **a**, **b** TIMP-2 (**a**) and periostin (**b**) are strongly detectable in the ECM of gingival tissues cultured in control medium. **c**, **d** Higher power view of the gingival tissue in **c** is presented in **d**. Periostin is not detectable in gingival tissue cultured in medium conditioned with anti-TIMP-2 antibody. **e–h** Higher power views of gingival tissues in **e**, **g** are presented in **f**, **h**, respectively. Neutralization of TIMP-1 (**e**, **f**) or TIMP-3 (**g**, **h**) does not alter the localization of periostin in gingival tissues. *Bars* 100 μm

tent. The typical ECM proteins in tendinous connective tissues, periodontal ligaments, and gingival tissues are types I and III collagens, tenascin-C, and fibronectin. A binding assay has shown that periostin binds to ECM proteins such as tenascin-C, fibronectin, collagen V, and periostin itself, but not to collagens I and III, and Fas-1 domains in periostin are responsible for these bindings (Takayama et al. 2006). On the other hand, an immunoelectron-microscopical analysis has suggested that periostin binds to type I collagen in periodontal ligaments in vivo (Kii et al. 2006). In contrast to periostin, no reports are available on binding assays of TIMP-2 to ECM components. Among the TIMP family, TIMP-3 is well known to have a specific ECM-binding domain and associates directly with heparan sulfate proteoglycans (Yu et al. 2000). Interestingly, the tissue distributions of TIMP-2 and TIMP-3 are significantly different in our study, emphasizing the role of TIMP-2 in tissues affected by mechanical strain. The binding mechanism of TIMP-2 to ECM components remains to be established. In our in vitro study, TIMP-2 is abundantly expressed in cultured P2 jaw mesenchyme (Fig. 8a); however, TIMP-2 is not detectable in cultured E14 jaw mesenchyme (data not shown). Furthermore, TIMP-2 expression in the ECM of periodontal ligaments is delayed compared with that of periostin. Thus, the maturation of collagen fibrils might be related to the binding of TIMP-2 to the ECM. The expression of TIMP-2 and periostin in the jaw mesenchyme is temporospatially regulated; the stained mesenchyme extends from the lingual to buccal areas and in an anterior to posterior direction and gives rise to gingival tissues. Developmental mechanisms of gingival tissues remain unknown, although the distribution of TIMP-2 and periostin might be related to gingival development. Although TIMP-2 and periostin are similarly distributed, their staining patterns are significantly different. TIMP-2 appears to be associated with the ECM from an early stage of development, whereas periostin shows a punctate pattern combined with fibrils. Recently, the association of periostin with Notch 1 has been reported (Tanabe et al. 2004); this might be related to its punctate expression.

ECM composition appears to be regulated by mechanical stresses placed on cells in connective tissues (Banes et al. 2001). Mechanical stress affects the expression of MMPs and TIMPs in various cell types (Bolcato-Bellemin et al. 2000; Tsuji et al. 2004; He et al. 2004). Stretch applied to periodontal ligaments and gingival fibroblasts induces the expression of *Mmp-1*, *Mmp-2*, *Timp-1*, and *Timp-2* mRNAs, whereas that of *Mt1-mmp* is not varied (Bolcato-Bellemin et al. 2000; He et al. 2004). Intermittent tensile stress to periodontal ligament cells increases the expression of *Timp-1* and *Timp-2* mRNAs, but barely affects that of *Mmp-1* and *Mmp-2* mRNA, suggesting that appropriate stress acts as an inhibitor of the degradation of ECM in the periodontal ligament (Tsuji et al. 2004). In rat tendon, MMP-2 and MT1-MMP, whose activities are strongly controlled by TIMP-2, have been shown to participate not only in collagen degradation, but also in collagen remodeling (Oshiro et al. 2003). In addition to its MMP inhibition activity, TIMP-2 can provoke a significant increase in fibroblast collagen synthesis (Lovelock et al. 2005). On the other hand, mechanical stress also alters *periostin* mRNA expression. Periostin expression increases under pressure from orthodontic tooth movement (Wilde et al. 2003) and decreases during occlusal hypofunction in the mouse periodontal ligament (Afanador et al. 2005). Periostin null mice placed on a soft diet that alleviates mechanical strain on the periodontal ligament show partial rescue of periodontal disease-like phenotypes (Rios et al. 2005). Furthermore, periostin has been suggested to digest collagen fibers in the shear zone of the mouse incisor periodontal ligament (Kii et al. 2006). Thus, TIMP-2 and periostin appear to play key roles in maintaining the

homeostasis of tissues receiving mechanical strain. MMPs can degrade all ECM components, although which MMPs can cleave periostin remain unknown. In our in vitro study, the localization patterns of periostin drastically alter in gingival tissues cultured in anti-TIMP-2 antibody-conditioned medium (Fig. 8c, d). In contrast, the addition of anti-TIMP-1 or anti-TIMP-3 antibodies does not affect periostin distribution (Fig. 8e–h). TIMP-2 may protect the degradation of periostin from MMP activities.

In addition to their similar tissue distributions, TIMP-2 and periostin have similar properties with regard to cellular behavior, and multiple reports have independently shown their close correlations with metastatic growth in cancer. Both proteins affect cytodifferentiation. TIMP-2 induces the differentiation of cardiac fibroblasts (Lovelock et al. 2005) and skeletal muscles (Lluri and Jaworski 2005), whereas periostin is correlated with smooth muscle cell differentiation (Lindner et al. 2005). TIMPs (Edwards et al. 1987; Overall et al. 1991) and periostin (Horiuchi et al. 1999) can be induced by TGF-β1, which is known to stimulate ECM protein synthesis via Smad proteins (Zhang et al. 2000; Arai et al. 2002; Lindahl et al. 2002). An association between TGF-β1 and mechanical loading has also been demonstrated in a number of cell and tissue types. Stretch-force-induced TGF-β1 expression has been shown in tendons (Skutek et al. 2001), cardiac fibroblasts (Ruwhof et al. 2000; Lindahl et al. 2002), and osteoblast-like cells (Klein-Nulend et al. 1995). Fibroblasts overexpressing TGF-β1 show increased TIMP-2 expression more significantly than other TIMPs, suggesting effects of TGF-β1 on the MMP/TIMP system (Seeland et al. 2002). TGF-β1 and its inducers, TIMP-2 and periostin, may coordinately function as ECM modulators in tissues that experience mechanical strain.

Integrin α3β1 appears to be the common integrin to which TIMP-2 (Seo et al. 2003) and periostin (Kudo et al. 2004) can bind. This has been confirmed in the early stages of molar tooth morphogenesis, at which time TIMP-2, periostin, and integrin α3 are all clearly detectable along the outer dental epithelium on the lingual side. In contrast, the buccal side is devoid of these proteins (Fig. 1d, e, h, i). On the contrary, laminin-5 (α3β3γ2), which is associated with several epithelial tissues, has been detected at a much higher intensity on the buccal side rather than the lingual side of the basement membrane at E14 (Yoshiba et al. 1998a). During normal developmental tissue growth, the basement membrane is subjected to increased mechanical strain. Local stress changes are suggested to control basement membrane remodeling by Rho, a small GTPase, and cytoskeletal tension (Moore et al. 2005; Ingber 2006). TIMP-2 promotes the association of Rap 1, the closest homolog of the small GTPase Ras, with actin (Chang et al. 2006). Rho and Ras signaling, which regulates the organization of the actin cytoskeleton, are involved in submandibular gland development through integrin α3β1 (Menko et al. 2001). Laminin-5 is also involved in epithelial morphogenesis (Baker et al. 1996; Stahl et al. 1997). The differential localization of these proteins on the dental basement membrane may indicate that the morphogenesis of molar teeth is asymmetrically regulated. In incisors, TIMP-2 and periostin have been specifically detected on the basement membrane of the apical loop (Fig. 6) from the early bell stage of development, at which time laminin-5 is also strongly detectable (Yoshiba et al. 1998b). Further studies should elucidate any interactive functions among these molecules on the basement membrane.

A novel constructor of tissue junctions, viz., collagen XXII, has recently been reported (Koch et al. 2004). Collagen XXII is strictly restricted to tissue junctions in muscles, tendons, heart, and articular cartilage. Notably, the immunostaining pattern of collagen XXII in hair follicles is surprisingly similar to that of periostin demonstrated in our study (Fig. 7c) in which collagen XXII and periostin have been found in the lower part of hair follicles with a sheath-like staining pattern. Periostin was originally identified as a homophilic adhesion molecule (Takeshita et al. 1993). Thus, the localization of both proteins suggests the presence of a junctional structure between multiple epithelial layers in hair follicles (Langbein et al. 2002).

In conclusion, TIMP-2 protein associates with the ECM of tissues that are exposed to mechanical forces, from early stages of development. Furthermore, the tissue distribution of TIMP-2 is strikingly similar to that of periostin. Both proteins also colocalize on the dental basement membrane during tooth morphogenesis, and their distribution patterns are asymmetrically and spatiotemporally regulated. Additional studies may determine their potential roles and functional relationships in ECM remodeling.

Acknowledgements The authors thank Prof. Dylan Edwards and Dr. Robert Nuttall (University of East Anglia, Norfolk, UK) for their generous gift of the cDNA for TIMP-2.

References

Afanador E, Yokozeki M, Oba Y, Kitase Y, Takahashi T, Kudo A, Moriyama K (2005) Messenger RNA expression of periostin and Twist transiently decrease by occlusal hypofunction in mouse periodontal ligament. Arch Oral Biol 50:1023–1031

Arai K, Kasashima Y, Kobayashi A, Kuwano A, Yoshihara T (2002) TGF-beta alters collagen XII and XIV mRNA levels in cultured equine tenocytes. Matrix Biol 21:243–250

Baker SE, Hopkinson SB, Fitchmun M, Andreason GL, Frasier F, Plopper G, Quaranta V, Jones JC (1996) Laminin-5 and hemidesmosomes: role of the alpha 3 chain subunit in hemidesmosome stability and assembly. J Cell Sci 109:2509–2520

Baker AH, Edwards DR, Murphy G (2002) Metalloproteinase inhibitors: biological actions and therapeutic opportunities. J Cell Sci 115:3719–3727

Banes AJ, Lee G, Graff R, Otey C, Archambault J, Tsukazi M, Elfervig M, Qi J (2001) Mechanical forces and signaling in connective tissue cells: cellular mechanisms of detection, transduction, and responses to mechanical deformation. Curr Opin Orthop 12:389–396

Bolcato-Bellemin AL, Elkaim R, Abehsera A, Fausser JL, Haikel Y, Tenenbaum H (2000) Expression of mRNAs encoding for alpha and beta integrin subunits, MMPs, and TIMPs in stretched human periodontal ligament and gingival fibroblasts. J Dent Res 79:1712–1716

Chang H, Lee J, Poo H, Noda M, Diaz T, Wei B, Stetler-Stevenson WG, Oh J (2006) TIMP-2 promotes cell spreading and adhesion via upregulation of Rap1 signaling. Biochem Biophys Res Commun 345:1201–1206

Edwards DR, Murphy G, Reynolds JJ, Whitham SE, Docherty AJ, Angel P, Heath JK (1987) Transforming growth factor beta modulates the expression of collagenase and metalloproteinase inhibitor. EMBO J 6:1899–1904

Gillan L, Matei D, Fishman DA, Gerbin CS, Karlan BY, Chang DD (2002) Periostin secreted by epithelial ovarian carcinoma is a ligand for alpha(V)beta(3) and alpha(V)beta(5) integrins and promotes cell motility. Cancer Res 62:5358–5364

Hayakawa T, Yamashita K, Ohuchi E, Shinagawa A (1994) Cell growth-promoting activity of tissue inhibitor of metalloproteinases-2 (TIMP-2). J Cell Sci 107:2373–2379

He Y, Macarak EJ, Korostoff JM, Howard PS (2004) Compression and tension: differential effects on matrix accumulation by periodontal ligament fibroblasts in vitro. Connect Tissue Res 45:28–39

Horiuchi K, Amizuka N, Takeshita S, Takamatsu H, Katsuura M, Ozawa H, Toyama Y, Bonewald LF, Kudo A (1999) Identification and characterization of a novel protein, periostin, with restricted expression to periosteum and periodontal ligament and increased expression by transforming growth factor beta. J Bone Miner Res 14:1239–1249

Ingber DE (2006) Mechanical control of tissue morphogenesis during embryological development. Int J Dev Biol 50:255–266

Kii I, Amizuka N, Minqi L, Kitajima S, Saga Y, Kudo A (2006) Periostin is an extracellular matrix protein required for eruption of incisors in mice. Biochem Biophys Res Commun 342:766–772

Kim JE, Kim SJ, Lee BH, Park RW, Kim KS, Kim IS (2000) Identification of motifs for cell adhesion within the repeated domains of transforming growth factor-beta-induced gene, beta ig-h3. J Biol Chem 275:30907–30915

Kim JE, Jeong HW, Nam JO, Lee BH, Choi JY, Park RW, Park JY, Kim IS (2002) Identification of motifs in the fasciclin domains of the transforming growth factor-beta-induced matrix protein beta ig-h3 that interact with the alphavbeta5 integrin. J Biol Chem 277:46159–46165

Klein-Nulend J, Roelofsen J, Sterck JG, Semeins CM, Burger EH (1995) Mechanical loading stimulates the release of transforming growth factor-beta activity by cultured mouse calvariae and periosteal cells. J Cell Physiol 163:115–119

Knauper V, Will H, Lopez-Otin C, Smith B, Atkinson SJ, Stanton H, Hembry RM, Murphy G (1996a) Cellular mechanisms for human procollagenase-3 (MMP-13) activation. Evidence that MT1-MMP (MMP-14) and gelatinase a (MMP-2) are able to generate active enzyme. J Biol Chem 271:17124–17131

Knauper V, Lopez-Otin C, Smith B, Knight G, Murphy G (1996b) Biochemical characterization of human collagenase-3. J Biol Chem 271:1544–1550

Koch M, Schulze J, Hansen U, Ashwodt T, Keene DR, Brunken WJ, Burgeson RE, Bruckner P, Bruckner-Tuderman L (2004) A novel marker of tissue junctions, collagen XXII. J Biol Chem 279:22514–22521

Kruzynska-Frejtag A, Wang J, Maeda M, Rogers R, Krug E, Hoffman S, Markwald RR, Conway SJ (2004) Periostin is expressed within the developing teeth at the sites of epithelial-mesenchymal interaction. Dev Dyn 229:857–868

Kudo H, Amizuka N, Araki K, Inohaya K, Kudo A (2004) Zebrafish periostin is required for the adhesion of muscle fiber bundles to the myoseptum and for the differentiation of muscle fibers. Dev Biol 267:473–487

Langbein L, Rogers MA, Praetzel S, Aoki N, Winter H, Schweizer J (2002) A novel epithelial keratin, hK6irs1, is expressed differentially in all layers of the inner root sheath, including specialized Huxley cells (Flugelzellen) of the human hair follicle. J Invest Dermatol 118:789–799

Leco KJ, Hayden LJ, Sharma RR, Rocheleau H, Greenberg AH, Edwards DR (1992) Differential regulation of TIMP-1 and TIMP-2 mRNA expression in normal and Ha-ras-transformed murine fibroblasts. Gene 117:209–217

Lindahl GE, Chambers C, Papakrivopoulou J, Dawson SJ, Jacobsen MC, Bishop JE, Laurent GJ (2002) Activation of fibroblast procollagen alpha 1(I) transcription by mechanical strain is transforming growth factor-beta-dependent and involves increased binding of CCAAT-binding factor (CBF/NF-Y) at the proximal promoter. J Biol Chem 277:6153–6161

Lindner V, Wang Q, Conley BA, Friesel RE, Vary CP (2005) Vascular injury induces expression of periostin: implications for vascular cell differentiation and migration. Arterioscler Thromb Vasc Bio 25:77–83

Lluri G, Jaworski DM (2005) Regulation of TIMP-2, MT1-MMP, and MMP-2 expression during C2C12 differentiation. Muscle Nerve 32:492–499

Lovelock JD, Baker AH, Gao F, Dong JF, Bergeron AL, McPheat W, Sivasubramanian N, Mann DL (2005) Heterogeneous effects of tissue inhibitors of matrix metalloproteinases on cardiac fibroblasts. Am J Physiol Heart Circ Physiol 288:461–468

Menko AS, Kreidberg JA, Ryan TT, Van Bockstaele E, Kukuruzinska MA (2001) Loss of alpha3beta1 integrin function results in an altered differentiation program in the mouse submandibular gland. Dev Dyn 220:337–349

Moore KA, Polte T, Huang S, Shi B, Alsberg E, Sunday ME, Ingber DE (2005) Control of basement membrane remodeling and epithelial branching morphogenesis in embryonic lung by Rho and cytoskeletal tension. Dev Dyn 232:268–281

Murphy AN, Unsworth EJ, Stetler-Stevenson WG (1993) Tissue inhibitor of metalloproteinases-2 inhibits bFGF-induced human microvascular endothelial cell proliferation. J Cell Physiol 157:351–358

Ohuchi E, Imai K, Fujii Y, Sato H, Seiki M, Okada Y (1997) Membrane type 1 matrix metalloproteinase digests interstitial collagens and other extracellular matrix macromolecules. J Biol Chem 272:2446–2451

Oshiro W, Lou J, Xing X, Tu Y, Manske PR (2003) Flexor tendon healing in the rat: a histologic and gene expression study. J Hand Surg 28:814–823

Overall CM, Wrana JL, Sodek J (1991) Transcriptional and post-transcriptional regulation of 72-kDa gelatinase/type IV collagenase by transforming growth factor-beta 1 in human fibroblasts. Comparisons with collagenase and tissue inhibitor of matrix metalloproteinase gene expression. J Biol Chem 266: 14064–14071

Rios H, Koushik SV, Wang H, Wang J, Zhou HM, Lindsley A, Rogers R, Chen Z, Maeda M, Kruzynska-Frejtag A, Feng JQ, Conway SJ (2005) Periostin null mice exhibit dwarfism, incisor enamel defects, and an early-onset periodontal disease-like phenotype. Mol Cell Biol 25:11131–11144

Ruwhof C, Wamel AE van, Egas JM, Laarse A van der (2000) Cyclic stretch induces the release of growth promoting factors from cultured neonatal cardiomyocytes and cardiac fibroblasts. Mol Cell Biochem 208:89–98

Sabeh F, Ota I, Holmbeck K, Birkedal-Hansen H, Soloway P, Balbin M, Lopez-Otin C, Shapiro S, Inada M, Krane S, Allen E, Chung D, Weiss SJ (2004) Tumor cell traffic through the extracellular matrix is controlled by the membrane-anchored collagenase MT1-MMP. J Cell Biol 167:769–781

Seeland U, Haeuseler C, Hinrichs R, Rosenkranz S, Pfitzner T, Scharffetter-Kochanek K, Bohm M (2002) Myocardial fibrosis in transforming growth factor-beta(1) (TGF-beta(1)) transgenic mice is associated with inhibition of interstitial collagenase. Eur J Clin Invest 32:295–303

Seiki M (2002) The cell surface: the stage for matrix metalloproteinase regulation of migration. Curr Opin Cell Biol 14:624–632

Seo DW, Li H, Guedez L, Wingfield PT, Diaz T, Salloum R, Wei BY, Stetler-Stevenson WG (2003) TIMP-2 mediated inhibition of angiogenesis: an MMP-independent mechanism. Cell 114:171–180

Skonier J, Bennett K, Rothwell V, Kosowski S, Plowman G, Wallace P, Edelhoff S, Disteche C, Neubauer M, Marquardt H, Rodgers J, Purchio AF (1994) Beta ig-h3: a transforming growth factor-beta-responsive gene encoding a secreted protein that inhibits cell attachment in vitro and suppresses the growth of CHO cells in nude mice. DNA Cell Biol 13:571–584

Skutek M, Griensven M van, Zeichen J, Brauer N, Bosch U (2001) Cyclic mechanical stretching modulates secretion pattern of growth factors in human tendon fibroblasts. Eur J Appl Physiol 86:48–52

Stahl S, Weitzman S, Jones JC (1997) The role of laminin-5 and its receptors in mammary epithelial cell branching morphogenesis. J Cell Sci 110:55–63

Suzuki H, Amizuka N, Kii I, Kawano Y, Nozawa-Inoue K, Suzuki A, Yoshie H, Kudo A, Maeda T (2004) Immunohistochemical localization of periostin in tooth and its surrounding tissues in mouse mandibles during development. Anat Rec 281:1264–1275

Takayama G, Arima K, Kanaji T, Toda S, Tanaka H, Shoji S, McKenzie AN, Nagai H, Hotokebuchi T, Izuhara K (2006) Periostin: a novel component of subepithelial fibrosis of bronchial asthma downstream of IL-4 and IL-13 signals. J Allergy Clin Immunol 118:8–104

Takeshita S, Kikuno R, Tezuka K, Amann E (1993) Osteoblast-specific factor 2: cloning of a putative bone adhesion protein with homology with the insect protein fasciclin I. Biochem J 294: 271–278

Tanabe H, Kii I, Amizuka N, Katsube K, Kudo A (2004) Notch signaling is activated by binding of periostin or CCN3 to Notch1 in osteoblasts. J Bone Miner Res 19:S275

Tsuji K, Uno K, Zhang GX, Tamura M (2004) Periodontal ligament cells under intermittent tensile stress regulate mRNA expression of osteoprotegerin and tissue inhibitor of matrix metalloprotease-1 and -2. J Bone Miner Metab 22:94–103

Wilde J, Yokozeki M, Terai K, Kudo A, Moriyama K (2003) The divergent expression of periostin mRNA in the periodontal ligament during experimental tooth movement. Cell Tissue Res 312:345–351

Yoshiba K, Yoshiba N, Aberdam D, Meneguzzi G, Perrin-Schmitt F, Stoetzel C, Ruch JV, Lesot H (1998a) Expression and localization of laminin-5 subunits during mouse tooth development. Dev Dyn 211:164–176

Yoshiba N, Yoshiba K, Aberdam D, Meneguzzi G, Perrin-Schmitt F, Stoetzel C, Ruch JV, Lesot H (1998b) Expression and localization of laminin-5 subunits in the mouse incisor. Cell Tissue Res 292:143–149

Yoshiba N, Yoshiba K, Stoetzel C, Perrin-Schmitt F, Cam Y, Ruch JV, Lesot H (2003) Temporospatial gene expression and protein localization of matrix metalloproteinases and their inhibitors during mouse molar tooth development. Dev Dyn 228:105–112

Yoshiba N, Yoshiba K, Stoetzel C, Perrin-Schmitt F, Cam Y, Ruch JV, Hosoya A, Ozawa H, Lesot H (2006) Differential regulation of TIMP-1, -2, and -3 mRNA and protein expressions during mouse incisor development. Cell Tissue Res 324:97–104

Yu WH, Yu S, Meng Q, Brew K, Woessner JF Jr (2000) TIMP-3 binds to sulfated glycosaminoglycans of the extracellular matrix. J Biol Chem 275:31226–31232

Zhang W, Ou J, Inagaki Y, Greenwel P, Ramirez F (2000) Synergistic cooperation between Sp1 and Smad3/Smad4 mediates transforming growth factor beta1 stimulation of alpha 2(I)-collagen (COL1A2) transcription. J Biol Chem 275:39237–39245

Differentiation (2007) 75:452–462 DOI: 10.1111/j.1432-0436.2006.00150.x

ORIGINAL ARTICLE

Takashi Yamashiro · Li Zheng · Yuko Shitaku · Masahiro Saito · Takanori Tsubakimoto · Kenji Takada · Teruko Takano-Yamamoto · Irma Thesleff

Wnt10a regulates dentin sialophosphoprotein mRNA expression and possibly links odontoblast differentiation and tooth morphogenesis

Received July 23, 2006; accepted in revised form October 13, 2006

Abstract We have explored the role of Wnt signaling in dentinogenesis of mouse molar teeth. We found that Wnt10a was specifically associated with the differentiation of odontoblasts and that it showed striking colocalization with dentin sialophosphoprotein (Dspp) expression in secretory odontoblasts. Dspp is a tooth specific non-collagenous matrix protein and regulates dentin mineralization. Transient overexpression of Wnt10 in C3H10T1/2, a pluripotent fibroblast cell line induced Dspp mRNA. Interestingly, this induction occurred only when transfected cells were cultured on Matrigel basement membrane extracts. These findings indicated that Wnt10a is an upstream regulatory molecule for Dspp expression, and that cell–matrix interaction is essential for induction of Dspp expression. Furthermore, Wnt10a was specifically expressed in the epithelial signaling centers regulating tooth development, the primary and secondary enamel knots. The spatial and temporal distribution of Wnt10a mRNA demonstrated that the expression shifts from the secondary enamel knots, to the underlying preodontoblasts in the tips of future cusps. The expression patterns and overexpression studies together indicate that Wnt10a is a key molecule for dentinogenesis and that it is associated with the cell–matrix interactions regulating odontoblast differentiation. We conclude that Wnt10a may link the differentiation of odontoblasts and cusp morphogenesis.

Key words odontoblast · Dspp · Wnt10a · dentinogenesis · tooth

Takashi Yamashiro · Yuko Shitaku · Kenji Takada
Department of Orthodontics and Dentofacial Orthopedics
Graduate School of Dentistry
Osaka University, 1-8 Yamadaoka, Suita
Osaka 565-0871, Japan

Takashi Yamashiro (✉) · Li Zheng · Teruko Takano-Yamamoto
Department of Orthodontics and Dentofacial Orthopedics
Graduate School of Medicine and Dentistry
Okayama University, 2-5-1 Shikata-cho
Okayama 700-8558, Japan
Tel: +81 86 2356690
Fax: +81 86 2356694
E-mail: yamataka@md.okayama-u.ac.jp

Takashi Yamashiro · Irma Thesleff
Developmental Biology Programme, Institute of Biotechnology, University of Helsinki, Helsinki 00014, Finland

Masahiro Saito · Takanori Tsubakimoto
Department of Oral Medicine
Division of Operative Dentistry and Endodontics
Kanagawa Dental College
82 Inaoka-cho, Yokosuka
Kanagawa 238-8580, Japan

Introduction

Dentin is one of the three mineralized tissues of the tooth, and it is produced by odontoblasts differentiating from dental papilla mesenchymal cells. Dentin is very similar to bone in its matrix protein composition. However, whereas bone remodels throughout postnatal life and participates in calcium homeostasis, dentin, once formed, does not undergo remodeling. On the other hand, it can respond to injury or stimulation by forming reparative dentin to protect the dental pulp (Linde and Goldberg, 1993). Unlike osteoblast differentiation, the differentiation of odontoblasts is regulated by epithelial–mesenchymal interactions, which instruct both tooth morphogenesis and cell differentiation (Thesleff et al., 1989, 1991; Thesleff and Aberg, 1999). Recombination experiments of the dissociated developing dental

tissues have shown that odontoblast differentiation is controlled by the inner dental epithelium (Ruch et al., 1982; Kollar, 1985; Thesleff et al., 1989). Odontoblasts are columnar polarized cells with eccentric nuclei and long cellular processes, and this cytological polarization specifically occurs in a single cell layer adjacent to the basement membrane of the inner dental epithelium (Linde and Goldberg, 1993). The terminal differentiation of odontoblasts is initiated during the bell stage of tooth morphogenesis at the sites of the future cusps (Lesot et al., 2001; Thesleff et al., 2001). The patterning of the cusps, on the other hand, is determined by the positions of the secondary enamel knots, epithelial signaling centers resembling other embryonic signaling centers, such as the notochord and the apical ectodermal ridge in limbs (Jernvall et al., 1994; Jernvall and Thesleff, 2000). The cells of the enamel knots are non-proliferative, and they express several signaling molecules. These signals may control the folding of the inner enamel epithelium and as odontoblast differentiation starts from the mesenchymal cells underlying enamel knots it has been suggested that signals from the secondary enamel knots may also determine the location and time of the onset of odontoblast terminal differentiation (Thesleff et al., 2001). However the molecular mechanisms of the induction of odontoblast differentiation have remained unknown.

Dentin and bone share many extracellular matrix proteins associated with mineralization such as dentin matrix protein 1, fibronectin, collagen type I, alkaline phosphatase, osteonectin, osteopontin, bone sialoprotein, bono-1, and osteocalcin (Tsukamoto et al., 1992; Nakashima et al., 1994; Shiba et al., 1998; James et al., 2004). Dentin sialophosphoprotein (Dspp) is a non-collagenous extracellular matrix protein that is specifically expressed by odontoblasts (D'Souza et al., 1997). Dspp is a phosphorylated parent protein that is cleaved post-translationally into two proteins: dentin sialoprotein (Dsp) and dentin phosphoprotein (Dpp) (Feng et al., 1998). *In situ* hybridization and other experimental analyses have shown that *Dspp* is expressed predominantly in odontoblasts, transiently in preameloblasts, and at low levels in osteoblasts (D'Souza et al., 1997; Qin et al., 2002). In humans, several mutations have been identified in patients with dentinogenesis imperfecta, which is an autosomal dominant disorder of the tooth that specifically affects dentin biomineralization (Shields et al., 1973; Xiao et al., 2001; Zhang et al., 2001; Rajpar et al., 2002). A similar phenotype is found in *Dspp* null mutant mice, which feature a disturbance of dentin mineralization without any influences on bone (Sreenath et al., 2003). Hence, it is established that Dspp has a crucial role in the formation of mineralized dentin. Although the importance of epithelial–mesenchymal interactions and extracellular matrix for odontoblast differentiation is established, the molecular mechanisms of the interactions mediating odontoblast differentiation and inducing *Dspp* expression are not known.

Wnt genes encode a large family of secreted signaling proteins that specify various cell lineage pathways in development. Wnt proteins are now recognized as one of the major families of developmentally important signaling molecules and they regulate such intriguing processes as embryonic induction, the generation of cell polarity, and the specification of cell fate (Cadigan and Nusse, 1997; Nusse, 2003). In early tooth development, several Wnt genes are expressed from the initiation stage to the early bell stage (Sarkar and Sharpe, 1999). Targeted inactivation of lymphoid enhancer factor-1 (LEF1), a nuclear mediator of Wnt signaling, results in an arrest of tooth development at the bud stage (van Genderen et al., 1994). LEF1 serves as a relay of a Wnt signal to a fibroblast growth factor signal in the enamel knot in the dental epithelium, which establishes a network of reciprocal and sequential signaling between epithelium and mesenchyme (Kratochwil et al., 2002).

Here we provide evidence that Wnt10a signaling may be involved in odontoblast terminal differentiation, and based on the expression pattern of *Wnt10a*, we suggest that it has a role in linking tooth morphogenesis and odontoblast differentiation.

Materials and methods

Materials

Lipofectamine Plus was obtained from Gibco BRL (Gaithersburg, MD). Biocoat Matrigel-coated dishes were from Becton Dickinson (Labware, MA). The rabbit polyclonal anti-Wnt10a antibody was produced by Sigma Genosys Co. (Hokkaido, Japan) using a synthetic peptide as antigen, which was established by the Wnt10a protein sequence analysis (U61969). The amino acid sequence of the antigen peptide is RRGDEEAFRRKLHR and corresponds to amino acids 163–176 of the Wnt10a protein. All other chemicals were analytical grade.

Processing of tissues

Wild-type mouse embryos were obtained from the NMRI strain. Heads of embryonic E12, E13, E14, and E16 mice and postnatal 14 day old mice were dissected in Dulbecco's phosphate-buffered saline. The tissues were fixed in 4% paraformaldehyde at 4°C overnight. P14 heads were decalcified in 12.5% ethylene-diamine-tetra-acetic acid (EDTA) for 3 weeks. They were dehydrated, embedded in paraffin and serially sectioned at 7 μm.

Probes and *in situ* hybridization

The mouse *Wnt10a* cDNA was kindly provided by Dr Andrew P. McMahon, Harvard University, Boston, MA. Mouse *Dspp* probes were generated from A 550 bp *Dspp* fragment spanning the region between 656 and 1205 in accession # NM010080. The preparation of Bmp3 RNA probes has previously been described (Åberg et al., 1997). *In situ* hybridization of paraffin sections using 35S-UTP-labeled riboprobe was performed as described previously (Vainio

et al., 1993). The bright field and dark field images of each section were digitized, and the grains from dark fields were selected, colored red, and added to the bright field pictures in PhotoShop 6 (Åberg et al., 1997). Keratin was used as a marker for epithelial cells and it was detected by immunohistochemistry using polyclonal pan-keratin antibodies (DAKO, A575, Glostrup, Denmark) (Yamashiro et al., 2003).

Cell cultures

C3T10T1/2 cell lines, derived from embryonic mouse mesenchyme, were obtained from Riken cell bank (Tsukuba, Japan). These cells were cultured in Dulbecco's modified Eagle's medium (D-MEM, high glucose (4,500 mg/l D-glucose), with L-glutamine, and phenol red) supplemented with 0.1 mM non-essential amino acids (NEAA), 10% fetal bovine serum (FBS), 100 units U/ml penicillin, 100 μg/ml streptomycin, and incubated at 37°C in a 5% carbon dioxide, 95% air, humidified atmosphere. The cells were subcultured every 3–4 days, using 0.05% (w/v) EDTA to detach cells from the culture dish.

Wnt10a transfection in C3T10T1/2 cells

Mammalian expression vectors encoding mouse Wnt10 were constructed for transient transfections. Full-length mouse *Wnt10a* cDNA (Wang and Shackleford, 1996), pj32 was kindly provided by Dr. Gregory M. Shackleford, University of Southern California, Los Angeles, CA. *Wnt10a* was transferred from pj32 to the multiple cloning site of pCMV-Script (Stratagene, La Jolla, CA) with the restriction sites *Eco*RI and *Xho*I to generate pCMV-Wnt10a. Cells (60%–80% confluence) were transiently transfected with Lipofectamine Plus reagent (Gibco BRL, Gaithersburg, MD) according to the manufacturer's instructions. Briefly, pCMV-Wnt10a was mixed with Plus reagent in Opti-MEM I and incubated at room temperature for 15 min. Lipofectamine was mixed with DNA plus reagent and incubated further at room temperature for 15 min. Then the Lipofectamine Plus cDNA complex was added to the cells and incubated at 37°C. The control cells received Lipofectamine Plus alone. After 5 hr of incubation, growth medium containing 20% FBS was added for a final concentration of 10% FBS. The cells were maintained for an additional 12 hr. One day after transfection, cells were plated on Matrigel-coated dishes (Biocoat, Becton Dickinson Labware, Bedford, MA) or conventional culture dishes (Falcon, Becton Dickinson Labware).

Western blot analysis of Wnt10a

Cell lysate proteins (10 μg) from transfected cells were separated using 7.5% sodium dodecyl sulfate-polyacrylamide gel electrophoresis (SDS-PAGE) and were electrophoretically transferred from gel to polyvinylidene difluoride membranes. To separate non-specific protein binding, the membranes were incubated in 10 mM Tris HCl, pH 7.5, 100 mM NaCl, and 0.1% Tween 20 (TBST) containing 3% blot-qualified bovine serum albumin for 1 hr. The membranes were incubated in TBST containing a 1:1,000 diluted anti-Wnt10a antibody (Sigma Genosys Co, Hokkaido, Japan). Wnt10a polyclonal rabbit antibody was produced by Sigma Genosys Co based on the Wnt10a sequence CRRGDEEAFRR KLHR. Wnt10a antibody recognizes a band of approximately 48 kDa that corresponds to the size of Wnt10a in Wnt10a-transfected cells, while mock-transfected cells gave no signal (Fig. 2B). This signal disappeared after preincubation of the antibody with excess antigenic peptide CRRGDEEAFRRKLHR indicating that the band is specific.

The membrane was washed twice for 15 min each with 0.1% TBST, and incubated for 45 min with the secondary antibody, horseradish peroxidase (HRP)Rabbit-conjugated goat anti-rabbit (Amersham, Amersham, UK). Bound antibodies were visualized by chemiluminescence using an ECL Western Immunoblotting Kit (Amersham).

Reverse-transcriptase polymerase chain reaction (RT-PCR) of *Dspp* and *Wnt10a*

To determine whether *Wnt10a* overexpression in C3H10T1/2 cells induces *Dspp* expression, real-time PCR amplification of *Dspp* was performed. Five, ten and fifteen days after transfection, total RNA was isolated using the RNeasy-kit (Qiagen, Valencia, CA) according to the manufacturer's instructions. First molar tooth germs of the mandible from day 1 postnatal mouse pups were dissected in Dulbecco's PBS under a stereomicroscope. Total RNA was also isolated from tooth germs using the RNeasy-kit (Qiagen). Total RNA (1 μg) was reverse transcribed in 20 μl of transcription buffer [75 mM KCl, 50 mM Tris/HCl pH 8.3, 10 mM dithiothreitol, 3 mM $MgCl_2$, 0.5 mM deoxyribonucleotide trisphosphate, 1 μg oligo(dT)18-adapter primer] with Superscript II reverse transcriptase (200 U) for 1 hr at 42°C. Presence of *Dspp* and *Wnt10a* mRNA was determined using the LightCycler System and the Faststart DNA Master SYBR Green I kit (both from Roche Diagnostics, Mannheim, Germany). PCRs were performed according to the manufacturer's instructions with 0.5 μm each of the respective forward and reverse primers, 4 mM $MgCl_2$, and 1 × Faststart DNA Master SYBR Green I mix in a total volume of 20 μl. Cycling conditions were as follows: 10 min at 94°C, followed by 40 cycles with 15 sec C at 94°C, 10 sec at 64°C and 45 sec at 72°C. Standard GAPDH RT-PCR was used as an internal control for an adequate PCR reaction (472 bp). The following primers were used: 5′-atagcaccaaccatgag gct-3′ and 5′-cttttgttgcctttgttggg-3′ for *Dspp* gene, 5′-aactttggcattgt ggaagg-3′ and 5′-ggtcctcagtgtagcccaag-3′ for *Wnt10a*, 5′-aactttggc attgtggaagg -3′ and 5′-ccctgttgctgtagccgtat-3′ for GAPDH gene. PCR primer set for Dspp was designed for controlling the genomic DNA contamination. Primers that span intron–exon boundaries amplify a product from contaminating DNA that includes the intron, making it larger than the expected cDNA product. The products from the reactions described above were also run on a 1% (w/v) agarose gel, to confirm that all products were of the correct length for the primers used. After amplification, melting curve analysis of the PCR product was used to differentiate between specific and non-specific amplification products. Melting curve was acquired by heating the product at 20°C/sec to 95°C, cooling it at 20°C/sec to 55°C for 30 sec, and slowly heating it at 0.1 μC/sec to 94°C under continuous fluorescence monitoring. Melting curve analysis was accomplished with LightCycler software.

Results

Expression of *Wnt10a* and *Dspp* in the developing root

We evaluated the mRNA expression of several Wnt genes during root development at postnatal day 14, and found that *Wnt10a* transcripts were specifically present in the dental mesenchymal cells lining the inner dentin surface (Fig. 1A). *Dspp* mRNA was specifically expressed in odontoblasts (Fig. 1B), as shown previously (D'Souza et al., 1997; Bleicher et al., 1999), and both *Wnt10a* and *Dspp* were absent in the dental papilla cells, osteoblasts and cementoblasts.

The epithelial root sheath is a two-cell layer sheet at the apical end of the growing root and it regulates root growth as well as odontoblast differentiation. The root sheath can be visualized by immunohistochemistry

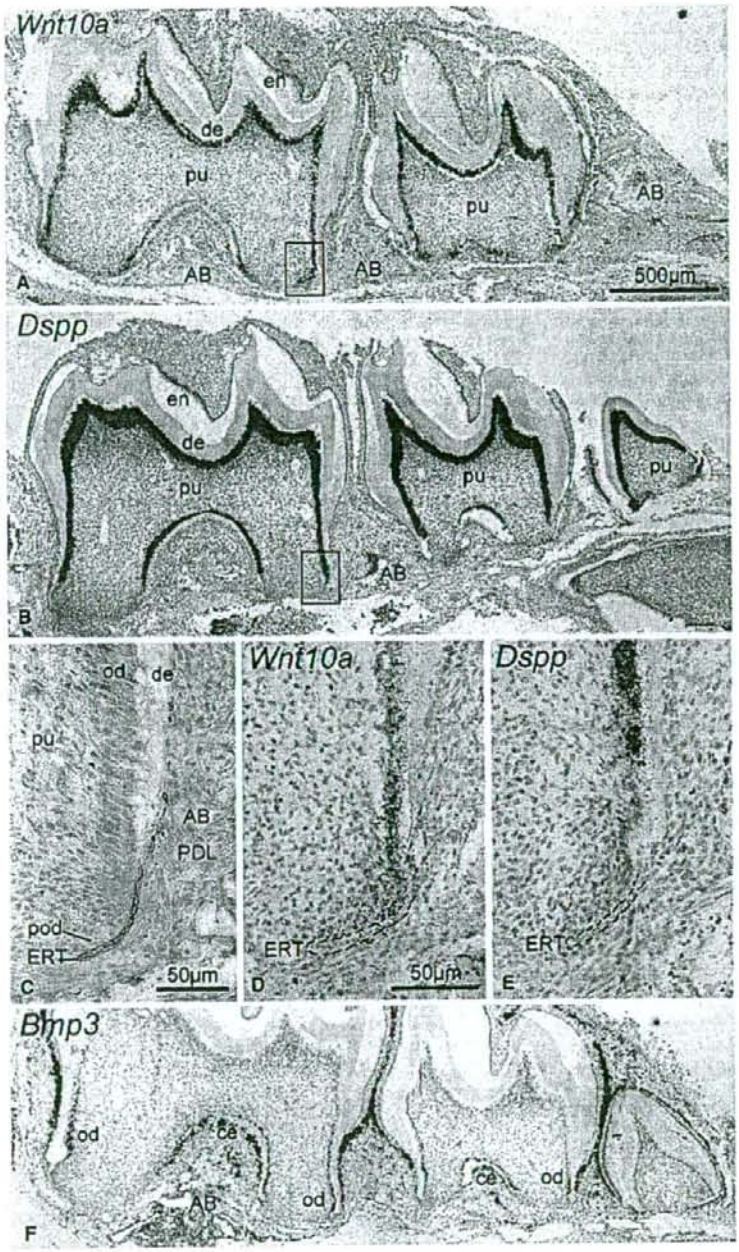

Fig. 1 Wnt10a and Dspp mRNA expression in lower jaw sections of a 14-days-old mouse (**A**, **B**) *Wnt10a* transcripts were specifically present in the odontoblasts lining the dentin (de) surface but not in the dental papilla cells (pu), or osteoblasts in the alveolar bone (AB). *Dspp* transcripts were also specifically present in odontoblasts. In higher magnification, the epithelial root sheath (ERT) is localized by immunohistochemistry using pan-keratin antibodies. Odontoblasts (od) are columnar cells lining the pulpal surface of dentin (de), and preodontoblasts (pod) are the odontoblast precursors in the apical end of the root. At the apical end of the growing root, *Wnt10a* transcripts were present in the preodontoblasts (pod). (**D**) The expression was continuous and maintained in differentiating and secretory odontoblasts (od). (**E**) *Dspp* expression was only detected in polarized odontoblasts (od). en, enamel; PDL, periodontal ligament. (**F**) Strong *Bmp3* expression was detected in cementoblasts the 1st and 2nd molars, as well as the dental follicle around all three molars. It was also observed in the osteoblasts on the active bone-forming surface.

using pan-keratin antibodies (Fig. 1C). Odontoblasts can be visualized as columnar cells lining the pulpal surface of dentin, and as the gradient of cell differentiation extends towards the root apex, preodontoblasts, i.e. the odontoblast precursors are present next to the root sheath (Fig. 1C). In higher magnification, *Wnt10a* transcripts were detected in differentiating and secretory odontoblasts and they were also diffusely present in the preodontoblasts underlying the epithelial root sheath (Fig. 1D). Previous reports showed that *Dspp* expres-

sion is initiated with matrix mineralization. *Dspp* was present in polarized odontoblasts but absent in preodontoblasts and differentiating odontoblasts indicating that the expression of *Wnt10a* precedes *Dspp* during the differentiation of the odontoblast cell lineage (Fig. 1E). At this stage, osteogenesis and cementogenesis were also active, as shown by intense *Bmp3* signals on the surfaces of bone and cementum (Fig. 1F) (Yamashiro et al., 2002). Hence, *Wnt10a* expression was expressed specifically in secretory odontoblasts

Wnt10a overexpression induces *Dspp* expression

As *Wnt10a* and *Dspp* transcripts overlapped in the odontoblasts but *Wnt10a* appeared earlier than *Dspp* in the odontoblast cell lineage, we hypothesized that Dspp might be induced by Wnt10a. To test this possibility, we overexpressed *Wnt10a* in the C310T1/2 cell line and examined its effect on *Dspp* expression. RT-PCR confirmed that C310T1/2 cells and Mock-transfected cells did not express *Wnt10a* mRNA, whereas *Wnt10a* transfected cells at 24 hr post-transfection and the cells derived from P1 tooth germs showed 340-bp bands of *Wnt10a* (Fig. 2A).

Induction of *Dspp* expression was detected in the *Wnt10a* transfected cells by real-time PCR ten days after transfection, but not after five or fifteen days. C3H10T1/2 cells did not show *Dspp* expression (Figs. 3A,3B). Gel electrophoresis of RT-PCR products (40 cycles) demonstrate a single band of 550 bp, corresponding to the *Dspp* transcript in cDNA derived from total RNA obtained from C310T1/2 cells transfected with pCMV-Wnt10a and cultured on Matrigel (Wnt10a Mg(+)), and positive control (tooth germ; Fig. 3B), indicating that *Dspp* induction was seen only when the cells were cultured on Matrigel coated dishes. Matrigel is an extract of basement membrane proteins (Kleinman et al., 1982 #16), and *Wnt10a* transfected cells cultured on conventional collagen coated dishes did not express *Dspp*. Mock transfected cells cultured on Matrigel dishes did not show *Dspp* expression (Figs. 3A,3B), indicating that Matrigel itself did not induce *Dspp*. These results indicated that Wnt10 can induce *Dspp* expression and that the specific basement membrane matrix was essential for this induction.

We confirmed the specificity of the amplified products and PCR products were not detected in Mock-transfected cells. The integrity of the RT-PCR products was confirmed by melting curve analysis (Fig. 3C). Melting curve analysis showed that the Tm of the *Dspp* templates was 88.5°C and occurred as a single amplicon peak for both *Wnt10a* transfected cells and control samples, reflecting the specificity of the PCR-products (Fig. 3C). The non-specific products, such as primer dimers, sometimes appeared, however, they melt below 80°C and were differentiated from the specific products by the melting curve analysis. These results were also confirmed by gel electrophoresis. Transfection and PCR were repeated three times.

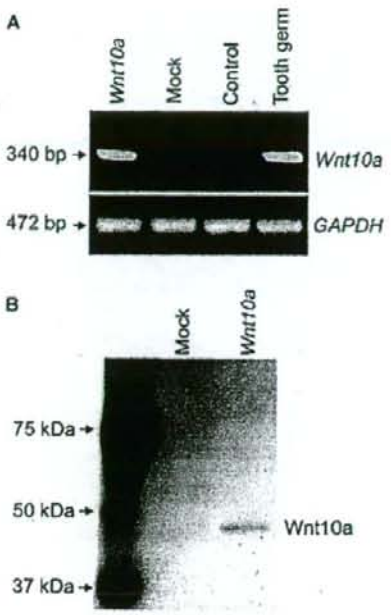

Fig. 2 C310T1/2 cells were transiently transfected with expression vectors encoding *Wnt10a*. (**A**) Expression of *Wnt10a* mRNA in C310T1/2 cells. After 24 hr transient transfection, total mRNA was extracted and submitted to reverse-transcriptase polymerase chain reaction (RT-PCR) using oligonucleotide primers specific of *Wnt10a* and *GAPDH*. Cells were transfected with pCMV-Wnt10a (Wnt10a) or its vehicle pCMV (Mock). Total RNA was also isolated from tooth germs and used as a positive control (tooth germ, 30 cycles). Negative control (control, 30 cycles) was performed in the absence of oligonucleotides. RT-PCR confirmed transfection efficiency using pCMV-WNT10a (Wnt10a, 30 cycles). (**B**) Expression of Wnt10a protein in C310T1/2 cells. Overexpression of Wnt10a protein was also confirmed by Western blot analysis 48 hr after transfection. Cells were lysed in sodium dodecyl sulfate-polyacrylamide gel electrophoresis (SDS-PAGE) loading buffer after transfection and analyzed by Western blot with specific antibodies to Wnt10a. pCMV-Wnt10-transfected (Wnt10a) cells showed Wnt10a protein expression. This protein expression was not observed in control cells transfected with vehicle pCMV (Mock). A molecular weight marker was run in parallel in the first lane.

Expression of *Wnt10a* during tooth development

At E14, the cap stage of tooth development, *Wnt10a* transcripts were intensely expressed in the enamel knot, as shown previously (Dassule and McMahon, 1998). No *Wnt10a* expression was detected in the dental mesenchyme (Fig. 4A). At E16, early bell stage, the primary enamel knot had disappeared, and *Wnt10a* was detected in secondary enamel knots. In addition, the mesenchymal cells directly underlying the enamel knots expressed *Wnt10a* (Fig. 4B). Subsequently at E18 transcripts were

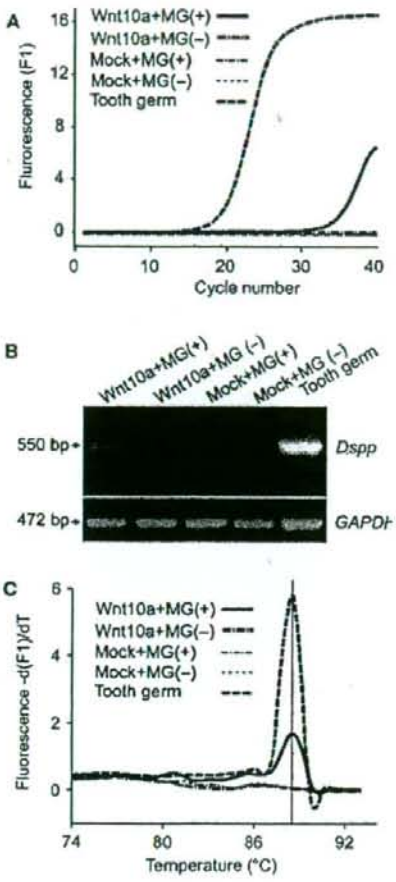

Fig. 3 Wnt10a transient transfection in C310T1/2 cells induced dentin sialophosphoprotein (Dspp) gene expression. (**A**) C310T1/2 cells were transiently transfected with pCMV-Wnt10a (Wnt10a) or its vehicle pCMV (Mock). Transfected cells were harvested 10 day post-transfection on Matrigel (Mg (+)) or collagen coated dishes (Mg (−)). Total mRNA extracted from the transfected cells was reverse transcribed and submitted to real-time polymerase chain reaction (PCR) using oligonucleotide primers specific of Dspp. Total RNA was also isolated from tooth germs and used as a positive control (Tooth germ). The *x*-axis denotes the cycle number of a quantitative PCR assay, and the y axis denotes the fluorescence intensity (F1) over the background. Amplification of Dspp was observed in C310T1/2 cells transfected with pCMV-Wnt10a and cultured on Matrigel (Wnt10a+Mg (+)), and positive control (tooth germ). (**B**) Forced-expression of Wnt10a induced Dspp expression when the transfected cells were cultured on Matrigel dishes (Wnt10a+Mg (+), 40 cycles). Wnt10a transfected cells cultured on normal culture dishes (Wnt10a+Mg (−), 40 cycles) and Mock transfected cells cultured on Matrigel dishes (Mock+Mg (+), 40 cycles) or normal culture dishes (Mock+Mg (−), 40 cycles) did not show Dspp expression. Positive control (Tooth germ) showed intense Dspp expression. (**C**) PCR products were subjected to melting peak analyses to determine the specificity of the products. Dspp sample showed a single product with Tm values of 88.5°C.

accumulated in the single cell layer of differentiating odontoblasts, which were aligned under the basement membrane (Fig. 4C). At E18, the differentiating odontoblasts became polarized and odontoblast differentiation initiated from the tips of the future cusps where the enamel knots are located (Fig. 5A). As the differentiation of preodontoblasts proceeded from the cusp tips in cervical direction along the cusp slopes *Wnt10a* expression was intimately linked with this gradient of differentiation. (Fig. 5B), and was highest in the cusp regions (Fig. 5C). *Dspp* expression was not yet expressed in the odontoblast lineage at this stage (Bleicher et al., 1999). In the early osteogenesis, *Wnt10a* was detected in the future bone regions at E13 and E14 (data not shown). This expression was down-regulated significantly at E16 and the expression could not be detected at P14 (Fig. 1A).

Discussion

The expression pattern of *Wnt10a* is associated with odontoblast differentiation

Our *in situ* hybridization analysis revealed that the expression of *Wnt10a* mRNA was associated with dentinogenesis. We found that *Wnt10a* expression was intense in the odontoblast cell layer and that it was maintained specifically in secretory odontoblasts where it was coexpressed with *Dspp*. In root development stage, mineralized matrix is also actively formed on the surface of bone and cementum, and the distribution of *Bmp3* expression indicated the regions of active osteogenesis and cementogenesis at the root surface and the surrounding alveolar bone surface. The comparison of *Wnt10a* and *Bmp3* distribution revealed that *Wnt10a* expression was specifically involved in odontogenesis, but not in osteogenesis or cementogenesis.

At the tip of the growing root, Hertwig's epithelial root sheath proliferates and directs root morphogenesis. The pulpal mesenchyme provides precursors for odontoblasts, and the subpopulation of pulp cells that contact the epithelial root sheath differentiate into preodontoblasts. As odontoblast differentiation is characterized by cytological polarization and they are lining in one cell layer they can be clearly distinguished from the surrounding pulpal cells. *In situ* hybridization analysis demonstrated that *Wnt10a* was not expressed in the pulpal mesenchyme, indicating that Wnt10a is induced when the precursor cells start to differentiate into odontoblasts.

Wnt10a regulates the expression of *Dspp*

Dspp and *Wnt10a* were colocalized in the differentiated odontoblasts. However, at the tip of the growing root,

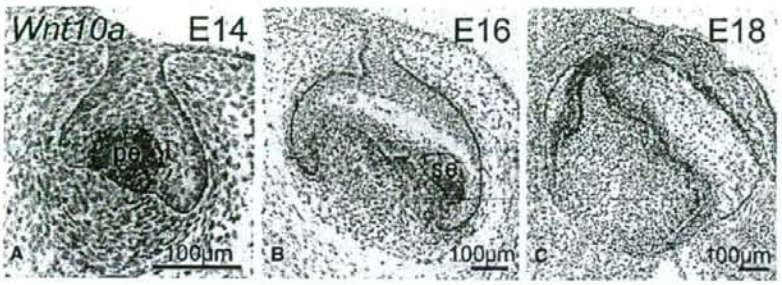

Fig. 4 At E14 (cap stage) *Wnt10a* transcripts were present in the primary enamel knot (pe), as shown previously. No expression was detected in the dental mesenchyme (A). At E16 (early bell stage) *Wnt10a* was detected in secondary enamel knots (se). In addition gene expression had shifted to the underlying mesenchymal cells (B). At E18 transcripts were accumulated in the single cell layer of differentiating odontoblasts (C).

Wnt10a expression was present in preodontoblasts beneath the epithelial sheath, but *Dspp* expression was absent indicating that *Wnt10a* expression appeared earlier than *Dspp* expression. Similarly, in early tooth development *Wnt10a* expression was first initiated in the odontogenic lineage cells at E14 whereas *Dspp* appeared in odontoblasts at E17 (Yamazaki et al., 1999). This temporo-spatial distribution pattern was in line with the possibility of an inductive role of *Wnt10a* on *Dspp* expression and we confirmed by transient overexpression of *Wnt10a* in C310T1/2 cells that Dspp was downstream of Wnt10a. The C310T1/2 cell line is derived from embryonic mesodermal cells, and can differentiate into distinctly different cell lineages, myoblasts, adipocytes, chondrocytes and osteoblasts under the influence of certain inducers (Taylor and Jones, 1979; Katagiri et al., 1990; Asahina et al., 1996). As C31010T1/2 cells did not constitutively express either *Wnt10a* or *Dspp* mRNA, our data indicated that *Dspp* was induced by Wnt10a in C31010T1/2 cells and that it may be a direct downstream target of Wnt10a (Fig. 6).

The extracellular mineralizing matrices of dentin and bone share many similarities, and it is likely that regulation of osteoblast and odontoblast differentiation may involve same signaling molecules (Thesleff et al., 2001). To our knowledge, Wnt10a is the first signal molecule that has specifically associated with odontoblast differentiation. Various Wnt genes, such as *Wnt1*, *Wnt4*, *Wnt5a*, *Wnt9a/14* and *Wnt7b*, are expressed in either osteoblast precursors or adjacent tissues during embryonic development, and *Wnt3a* and *Wnt10b* are expressed in bone marrow (Hartmann, 2006). In our study, we also demonstrated that *Wnt10a* was expressed in the future bone regions, but its expression was not maintained in the postnatal bone. Among these Wnt molecules, *Wnt10b* mutants display a postnatal decrease in bone mass and serum osteocalcin level, indicating that Wnt10b is an endogenous regulator of bone formation (Bennett et al., 2005). Wnt10b is homologous to Wnt10a, and WNT6 and WNT10a genes are clustered in tail-to-head manner. Like *Wnt10a*, both *Wnt10b* and *Wnt6* are expressed in the enamel knot and the dental epithelium in early tooth development (Dassule and McMahon, 1998; Sarkar and Sharpe, 1999). However, during later tooth development, *Wnt6* or *Wnt10b* transcripts were not detected in the odontoblast cell lineage by *in situ* hybridization (data not shown).

Cell to matrix interactions are required for the induction of *Dspp* expression by Wnta10a

Studies in the 1970's and 1980's showed that odontoblast differentiation depends on contacts between the

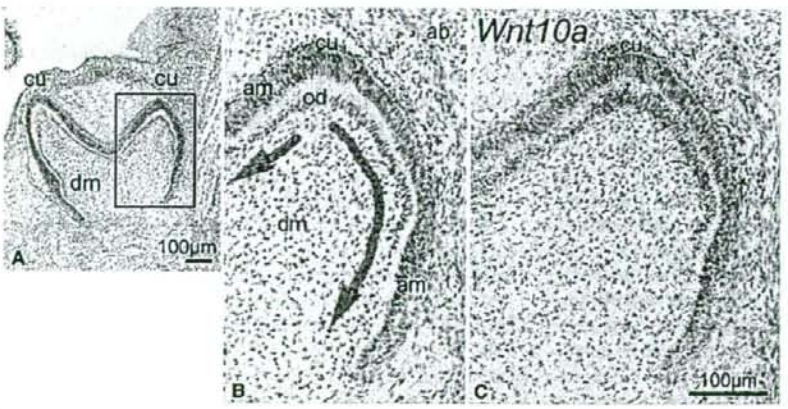

Fig. 5 Coronal sections of E18 molar (late bell stage) (A). (B) Higher magnification of the labial half of 1st molar (inset in panel A). Odontoblast differentiation has initiated beneath the forming cusp (cu) and the cells have polarized. (C). Wnt10a expression is associated with the gradient of odontoblast cytodifferentiation, and is highest in the cusp regions (cu).

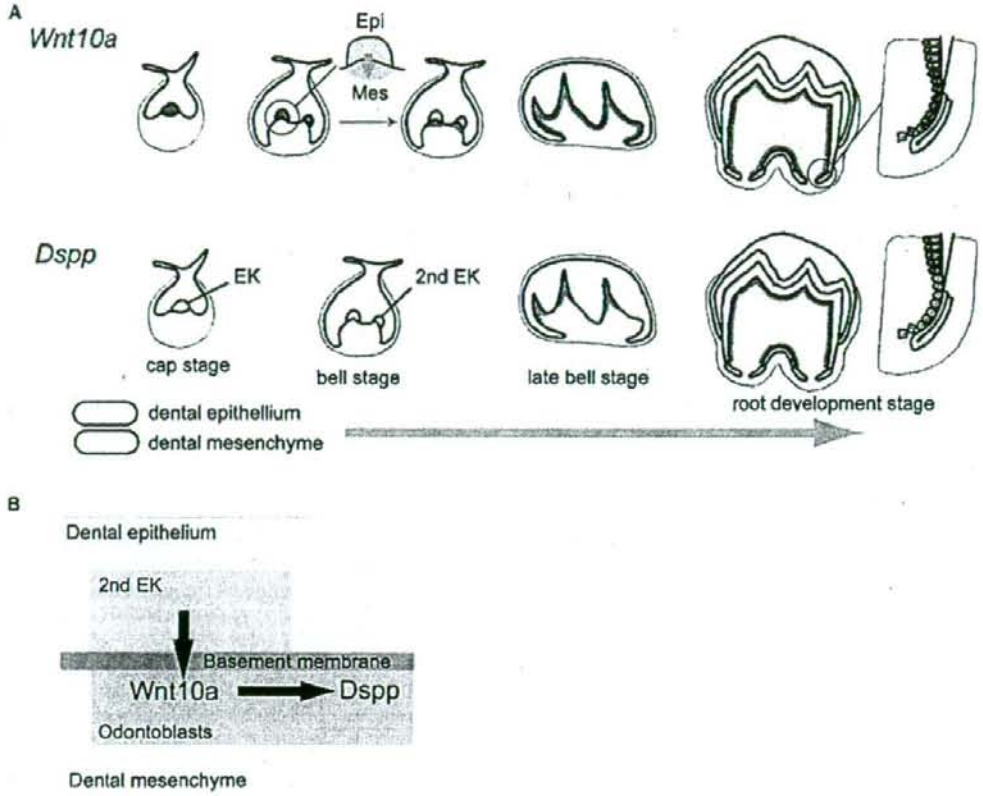

Fig. 6 (**A**) Summary of the expression of *Wnt10a* and *Dspp* during tooth development. *Wnt10a* is expressed in the enamel knot (EK) at the cap stage. At the bell stage, *Wnt10a* is expressed in the secondary enamel knot (2nd EK), and the expression has shifted to the underlying mesenchyme. In the late bell stages, *Wnt10a* expression is continuous in the preodontoblasts and odontoblasts. *Dspp* is expressed in the odontoblasts in the cusp regions. During root development, both *Wnt10a* and *Dspp* expression domains overlap in the odontoblasts. However, *Wnt10a* expression appeared earlier in the differentiating preodontoblasts underlying the epithelial root sheath. (**B**) Schematic diagram illustrating induction of *Dspp* expression by Wnt10a signals in the odontoblast cell lineage. *Wnt10a* appears in the mesenchymal cells beneath the secondary enamel knots. Wnt10a induces *Dspp* expression in the odontoblasts, and cell to matrix interactions are required for the induction of *Dspp* expression by Wnta10a. Hence, Wnt10a links tooth morphogenesis and odontoblast differentiation.

mesenchymal cells and the basement membrane underlining the enamel epithelium (Thesleff and Hurmerinta, 1981). Many extracellular matrix molecules were implicated in the cell–matrix interactions including fibronectin and other glycoproteins as well as proteoglycans. It was also suggested that growth factors and other diffusible molecules may have been trapped in the basement membrane, and involved in communication between cells. Interestingly, *Dspp* was induced only when the *Wnt10a*-transfected cells were cultured on Matrigel, which is an extract of basement membrane proteins (Kleinman et al., 1982), supporting the idea that cell to matrix association plays some role in odontoblast differentiation. As Mock-transfected cell did not show *Dspp* expression on Matrigel, Matrigel itself cannot induce odontogenesis. Among various molecules in the basement membrane, laminin alfa2 is subunit of laminin-2. Laminin-α2 deficiency resulted in a dramatic decrease in *Dspp* expression in odontoblasts (Yuasa et al., 2004), which is in agreement with our data and also supports the idea that cell–matrix interaction is essential for Dspp expression.

Heparan sulfate proteoglycans are major components of the extracellular matrix and regulate the transmission of developmental signals (Hacker et al., 2005). They also modulate the Wnt pathway (Haerry et al., 1997). In tooth development, odontoblast differentiation was inhibited *in vitro* by tunicamycin, which inhibited protein glycosylation and the accumulation of proteoglycans and glycoproteins in the basement mem-

brane of the developing tooth (Thesleff and Pratt, 1980). In tooth development also the cell surface proteoglycan syndecan-1 is involved in epithelial–mesenchymal interactions (Vainio et al., 1989; Thesleff et al., 1991), and syndecan-3 has been detected in the odontoblast layer underlying the inner enamel epithelium (Hikake et al., 2003). Heparin-sulfated forms of proteoglycans (HSPG) are long proteins with branched sugar side chains that are expressed on the cell surface, and can form complexes with a variety of signaling molecules, including Wnts and fibroblast growth factors (Nybakken and Perrimon, 2002). Hence it is possible that Wnt10a can be captured in the basement membrane extracellular matrix molecules to control differentiation of the pulp cells into odontoblasts. In addition, spatial distribution patterns of *Wnt10a* mRNA expression, together with previous findings, might provide an insight into a possible association between Wnt signaling and heparan sulfate proteoglycan in dentinogenesis. With tooth development, the basement membrane degrades and odontoblasts come into contact with the predentin surface. As predentin also contains various extracellular matrix molecules, such as proteoglycan and fibronectin (Linde and Goldberg, 1993), the cell–matrix interaction between odontoblasts and predentin might thus be explained the continuous expression of Wnt10a and Dspp in odontoblasts after the basement membrane has disappeared.

In our study, transfected cells were cultured on Matrigel in the medium supplemented with serum. Although both serum and Matrigel contain many growth factors and proteins these did not induce odontoblast differentiation as shown by the lack of *Dspp* expression in Mock transfected cells. Our real-time PCR data demonstrated that the *Dspp* induction by forced overexpression of *Wnt10a* was specific.

Odontoblast differentiation is regulated by reciprocal epithelial mesenchymal interactions. In addition, Dspp is expressed in a time- and site-specific manner and Dspp-expressing odontoblasts lie in one cell layer. These findings suggest that Dspp expression could be regulated by several inhibitory and stimulatory factors in a coordinated manner. Our real-time PCR data showed that Dspp induction in Wnt10a transfected-non-odontogenic cells was much less than the Dspp expression in intact odontoblasts. These data suggested that Wnt10a thus plays an important role in Dspp induction, however, further interaction with other putative molecules might be necessary to express a sufficient amount of Dspp during odontoblast differentiation.

Wnt10a and tooth morphogenesis

In the early tooth, *Wnt10a* is expressed in the enamel knot (Dassule and McMahon, 1998), which has a central function in the control of growth and patterning of the tooth crown (Jernvall and Thesleff, 2000; Miletich and Sharpe, 2003). Our *in situ* hybridization analysis showed that *Wnt10a* expression was reiterated in the secondary enamel knots which express most of the same signal molecules as the primary enamel knots and initiate cusp formation (Fig. 6A) (Vaahtokari et al., 1996). Interestingly, we found that *Wnt10a* expression shifted from the secondary enamel knots to the underlying mesenchyme. It could be that mesenchymal *Wnt10a* expression was induced by signaling molecules of the secondary enamel knots, perhaps by Wnt10a itself. The continuous *Wnt10a* mRNA distribution pattern in the odontoblasts suggested autocrine regulation of *Wnt10a* expression in the mesenchymal cells after the initial induction of *Wnt10a* by the epithelium.

Our study has provided new insight into the molecular mechanisms that spatially and temporally control the initiation of odontoblast differentiation. The terminal differentiation of odontoblasts is initiated at the tip of each cusp, indicating that the cell fate decision and morphogenesis is tightly linked (Fig. 6B). As both the initiation of odontoblast differentiation and the initiation of cusps coincide temporally and spatially with the secondary enamel knots, and as both processes are induced by epithelial signals (Jernvall et al., 1994; Jernvall and Thesleff, 2000), it is conceivable that some signals could regulate both cell differentiation as cusp morphogenesis. Our observations indicated that the expression of Wnt10a was intimately linked with the secondary enamel knots and the gradient of cytodifferentiation propagating apically from each cusp tip. Our data clearly demonstrated that *Wnt10a*-shifting from the epithelial signaling center to the underlying mesenchyme temporally and spatially corresponds to the initiation of odontoblast differentiation. In addition, functional network of Wnt10a and the cell to matrix interactions may trigger and regulate tooth specific *Dspp* expression. Putative matrix molecules may provide the cues for polarization of the cells, which may be necessary also for the transmission of the Wnt10a signal from the epithelium to the preodontoblast.

In summary, we found that *Wnt10a* was specifically expressed in the odontoblast cell lineage in mouse molars with striking colocalization with *Dspp* mRNA expression in the fully differentiated secretory odontoblasts. Dspp is a key molecule for dentin mineralization, and we showed that the forced expression of *Wnt10a* induced *Dspp* mRNA in pluripotent fibroblast cells, indicating that Wnt10a is possibly involved in dentine mineralization as an upstream regulator of Dspp. However, our observation that *Dspp* was induced only when the transfected cells were cultured on Matrigel suggests that cell to matrix interactions have crucial roles in dentinogenesis in conjunction with Wnt10a. This supports earlier proposals that odontoblast differentiation requires interactions between the mesenchymal cells and the extracellular matrix. We also found

that *Wnt10a* was expressed in the epithelial secondary enamel knots, and that this expression shifted to the underlying mesenchymal cells. The timing and location of this shift corresponds to the initiation of the polarization of preodontoblasts. Taken together, our findings indicate that Wnt10a and cell to matrix interactions play an important role for odontoblast differentiation and that Wnt10a links tooth morphogenesis and the differentiation of odontoblasts.

Acknowledgments We thank Merja Mäkinen and Riikka Santalahti for their excellent technical assistance. This study was supported by Grants-in-Aid for Scientific Research from the Japan Society for the Promotion of Science, the Academy of Finland, and the Sigrid Juselius Foundation.

References

Åberg, T., Wozney, J. and Thesleff, I. (1997) Expression patterns of bone morphogenetic proteins (Bmps) in the developing mouse tooth suggest roles in morphogenesis and cell differentiation. Dev Dyn 210:383–396.

Asahina, I., Sampath, T.K. and Hauschka, P.V. (1996) Human osteogenic protein-1 induces chondroblastic, osteoblastic, and/or adipocytic differentiation of clonal murine target cells. Exp Cell Res 222:38–47.

Bennett, C.N., Longo, K.A., Wright, W.S., Suva, L.J., Lane, T.F., Hankenson, K.D. and MacDougald, O.A. (2005) Regulation of osteoblastogenesis and bone mass by Wnt10b. Proc Natl Acad Sci USA 102:3324–3329.

Bleicher, F., Couble, M.L., Farges, J.C., Couble, P. and Magloire, H. (1999) Sequential expression of matrix protein genes in developing rat teeth. Matrix Biol 18:133–143.

Cadigan, K.M. and Nusse, R. (1997) Wnt signaling: a common theme in animal development. Genes Dev 11:3286–3305.

Dassule, H.R. and McMahon, A.P. (1998) Analysis of epithelial–mesenchymal interactions in the initial morphogenesis of the mammalian tooth. Dev Biol 202:215–227.

D'Souza, R.N., Cavender, A., Sunavala, G., Alvarez, J., Ohshima, T., Kulkarni, A.B. and MacDougall, M. (1997) Gene expression patterns of murine dentin matrix protein 1 (Dmp1) and dentin sialophosphoprotein (DSPP) suggest distinct developmental functions in vivo. J Bone Miner Res 12:2040–2049.

Feng, J.Q., Luan, X., Wallace, J., Jing, D., Ohshima, T., Kulkarni, A.B., D'Souza, R.N., Kozak, C.A. and MacDougall, M. (1998) Genomic organization, chromosomal mapping, and promoter analysis of the mouse dentin sialophosphoprotein (Dspp) gene, which codes for both dentin sialoprotein and dentin phosphoprotein. J Biol Chem 273:9457–9464.

Hacker, U., Nybakken, K. and Perrimon, N. (2005) Heparan sulphate proteoglycans: the sweet side of development. Nat Rev Mol Cell Biol 6:530–541.

Haerry, T.E., Heslip, T.R., Marsh, J.L. and O'Connor, M.B. (1997) Defects in glucuronate biosynthesis disrupt Wingless signaling in Drosophila. Development 124:3055–3064.

Hartmann, C. (2006) A Wnt canon orchestrating osteoblastogenesis. Trends Cell Biol 16:151–158.

Hikake, T., Mori, T., Iseki, K., Hagino, S., Zhang, Y., Takagi, H., Yokoya, S. and Wanaka, A. (2003) Comparison of expression patterns between CREB family transcription factor OASIS and proteoglycan core protein genes during murine tooth development. Anat Embryol (Berlin) 206:373–380.

James, M.J., Jarvinen, E. and Thesleff, I. (2004) Bonol: a gene associated with regions of deposition of bone and dentine. Gene Expr Patterns 4:595–599.

Jernvall, J., Kettunen, P., Karavanova, I., Martin, L.B. and Thesleff, I. (1994) Evidence for the role of the enamel knot as a control center in mammalian tooth cusp formation: non-dividing cells express growth stimulating Fgf-4 gene. Int J Dev Biol 38:463–469.

Jernvall, J. and Thesleff, I. (2000) Reiterative signaling and patterning during mammalian tooth morphogenesis. Mech Dev 92:19–29.

Katagiri, T., Yamaguchi, A., Ikeda, T., Yoshiki, S., Wozney, J.M., Rosen, V., Wang, E.A., Tanaka, H., Omura, S. and Suda, T. (1990) The non-osteogenic mouse pluripotent cell line, C3H10T1/2, is induced to differentiate into osteoblastic cells by recombinant human bone morphogenetic protein-2. Biochem Biophys Res Commun 172:295–299.

Kleinman, H.K., McGarvey, M.L., Liotta, L.A., Robey, P.G., Tryggvason, K. and Martin, G.R. (1982) Isolation and characterization of type IV procollagen, laminin, and heparan sulfate proteoglycan from the EHS sarcoma. Biochemistry 21: 6188–6193.

Kollar, E.J. (1985) Tissue interactions in development of teeth and related ectodermal derivatives. Dev Biol (NewYork) 4: 297–313.

Kratochwil, K., Galceran, J., Tontsch, S., Roth, W. and Grosschedl, R. (2002) FGF4, a direct target of LEF1 and Wnt signaling, can rescue the arrest of tooth organogenesis in Lef1(−/−) mice. Genes Dev 16:3173–3185.

Lesot, H., Lisi, S., Peterkova, R., Peterka, M., Mitolo, V. and Ruch, J.V. (2001) Epigenetic signals during odontoblast differentiation. Adv Dent Res 15:8–13.

Linde, A. and Goldberg, M. (1993) Dentinogenesis. Crit Rev Oral Biol Med 4:679–728.

Miletich, I. and Sharpe, P.T. (2003) Normal and abnormal dental development. Hum Mol Genet 12(Spec No 1): R69–R73.

Nakashima, M., Nagasawa, H., Yamada, Y. and Reddi, A.H. (1994) Regulatory role of transforming growth factor-beta, bone morphogenetic protein-2, and protein-4 on gene expression of extracellular matrix proteins and differentiation of dental pulp cells. Dev Biol 162:18–28.

Nusse, R. (2003) Wnts and Hedgehogs: lipid-modified proteins and similarities in signaling mechanisms at the cell surface. Development 130:5297–5305.

Nybakken, K. and Perrimon, N. (2002) Heparan sulfate proteoglycan modulation of developmental signaling in Drosophila. Biochim Biophys Acta 1573:280–291.

Qin, C., Brunn, J.C., Cadena, E., Ridall, A., Tsujigiwa, H., Nagatsuka, H., Nagai, N. and Butler, W.T. (2002) The expression of dentin sialophosphoprotein gene in bone. J Dent Res 81:392–394.

Rajpar, M.H., Koch, M.J., Davies, R.M., Mellody, K.T., Kielty, C.M. and Dixon, M.J. (2002) Mutation of the signal peptide region of the bicistronic gene DSPP affects translocation to the endoplasmic reticulum and results in defective dentine biomineralization. Hum Mol Genet 11:2559–2565.

Ruch, J.V., Lesot, H., Karcher-Djuricic, V., Meyer, J.M. and Olive, M. (1982) Facts and hypotheses concerning the control of odontoblast differentiation. Differentiation 21:7–12.

Sarkar, L. and Sharpe, P.T. (1999) Expression of Wnt signalling pathway genes during tooth development. Mech Dev 85:197–200.

Shiba, H., Fujita, T., Doi, N., Nakamura, S., Nakanishi, K., Takemoto, T., Hino, T., Noshiro, M., Kawamoto, T., Kurihara, H. and Kato, Y. (1998) Differential effects of various growth factors and cytokines on the syntheses of DNA, type I collagen, laminin, fibronectin, osteonectin/secreted protein, acidic and rich in cysteine (SPARC), and alkaline phosphatase by human pulp cells in culture. J Cell Physiol 174:194–205.

Shields, E.D., Bixler, D. and el-Kafrawy, A.M. (1973) A proposed classification for heritable human dentine defects with a description of a new entity. Arch Oral Biol 18:543–553.

Sreenath, T., Thyagarajan, T., Hall, B., Longenecker, G., D'Souza, R., Hong, S., Wright, J.T., MacDougall, M., Sauk, J. and

Kulkarni, A.B. (2003) Dentin sialophosphoprotein knockout mouse teeth display widened predentin zone and develop defective dentin mineralization similar to human dentinogenesis imperfecta type III. J Biol Chem 278:24874–24880.

Taylor, S.M. and Jones, P.A. (1979) Multiple new phenotypes induced in 10T1/2 and 3T3 cells treated with 5-azacytidine. Cell 17:771–779.

Thesleff, I. and Aberg, T. (1999) Molecular regulation of tooth development. Bone 25:123–125.

Thesleff, I. and Hurmerinta, K. (1981) Tissue interactions in tooth development. Differentiation 18:75–88.

Thesleff, I. and Pratt, R.M. (1980) Tunicamycin inhibits mouse tooth morphogenesis and odontoblast differentiation in vitro. J Embryol Exp Morphol 58:195–208.

Thesleff, I., Keranen, S. and Jernvall, J. (2001) Enamel knots as signaling centers linking tooth morphogenesis and odontoblast differentiation. Adv Dent Res 15:14–18.

Thesleff, I., Partanen, A.M. and Vainio, S. (1991) Epithelial–mesenchymal interactions in tooth morphogenesis: the roles of extracellular matrix, growth factors, and cell surface receptors. J Craniofac Genet Dev Biol 11:229–237.

Thesleff, I., Vainio, S. and Jalkanen, M. (1989) Cell–matrix interactions in tooth development. Int J Dev Biol 33:91–97.

Tsukamoto, Y., Fukutani, S., Shin-Ike, T., Kubota, T., Sato, S., Suzuki, Y. and Mori, M. (1992) Mineralized nodule formation by cultures of human dental pulp-derived fibroblasts. Arch Oral Biol 37:1045–1055.

Vaahtokari, A., Aberg, T., Jernvall, J., Keranen, S. and Thesleff, I. (1996) The enamel knot as a signaling center in the developing mouse tooth. Mech Dev 54:39–43.

Vainio, S., Jalkanen, M. and Thesleff, I. (1989) Syndecan and tenascin expression is induced by epithelial–mesenchymal interactions in embryonic tooth mesenchyme. J Cell Biol 108: 1945–1953.

Vainio, S., Karavanova, I., Jowett, A. and Thesleff, I. (1993) Identification of BMP-4 as a signal mediating secondary induction between epithelial and mesenchymal tissues during early tooth development. Cell 75:45–58.

van Genderen, C., Okamura, R.M., Farinas, I., Quo, R.G., Parslow, T.G., Bruhn, L. and Grosschedl, R. (1994) Development of several organs that require inductive epithelial–mesenchymal interactions is impaired in LEF-1-deficient mice. Genes Dev 8:2691–2703.

Wang, J. and Shackleford, G.M. (1996) Murine Wnt10a and Wnt10b: cloning and expression in developing limbs, face and skin of embryos and in adults. Oncogene 13:1537–1544.

Xiao, S., Yu, C., Chou, X., Yuan, W., Wang, Y., Bu, L., Fu, G., Qian, M., Yang, J., Shi, Y., Hu, L., Han, B., Wang, Z., Huang, W., Liu, J., Chen, Z., Zhao, G. and Kong, X. (2001) Dentinogenesis imperfecta 1 with or without progressive hearing loss is associated with distinct mutations in DSPP. Nat Genet 27: 201–204.

Yamashiro, T., Tummers, M. and Thesleff, I. (2003) Expression of bone morphogenetic proteins and Msx genes during root formation. J Dent Res 82:172–176.

Yamazaki, H., Kunisada, T., Miyamoto, A., Tagaya, H. and Hayashi, S. (1999) Tooth-specific expression conferred by the regulatory sequences of rat dentin sialoprotein gene in transgenic mice. Biochem Biophys Res Commun 260:433–440.

Yuasa, K., Fukumoto, S., Kamasaki, Y., Yamada, A., Fukumoto, E., Kanaoka, K., Saito, K., Harada, H., Arikawa-Hirasawa, E., Miyagoe-Suzuki, Y., Takeda, S., Okamoto, K., Kato, Y. and Fujiwara, T. (2004) Laminin alpha2 is essential for odontoblast differentiation regulating dentin sialoprotein expression. J Biol Chem 279:10286–10292.

Zhang, X., Zhao, J., Li, C., Gao, S., Qiu, C., Liu, P., Wu, G., Qiang, B., Lo, W.H. and Shen, Y. (2001) DSPP mutation in dentinogenesis imperfecta Shields type II. Nat Genet 27:151–152.

THE JOURNAL OF BIOLOGICAL CHEMISTRY VOL. 282, NO. 32, pp. 23070–23080, August 10, 2007

PLAP-1/Asporin, a Novel Negative Regulator of Periodontal Ligament Mineralization*[S]

Received for publication, December 6, 2006, and in revised form, May 7, 2007 Published, JBC Papers in Press, May 23, 2007, DOI 10.1074/jbc.M611181200

Satoru Yamada[‡], Miki Tomoeda[‡], Yasuhiro Ozawa[‡], Shinya Yoneda[‡], Yoshimitsu Terashima[‡], Kazuhiko Ikezawa[‡], Shiro Ikegawa[§], Masahiro Saito[¶], Satoru Toyosawa[‖], and Shinya Murakami[‡1]

From the Departments of [‡]Periodontology and [‖]Oral Pathology, Osaka University Graduate School of Dentistry, Suita, Osaka 565-0871, Japan, [§]Laboratory for Bone and Joint Disease, Single Nucleotide Polymorphisms Research Center, The Institute of Physical and Chemical Research (RIKEN), Minato-ku, Tokyo 108-8639, Japan, and [¶]Department of Oral Medicine, Division of Operative Dentistry and Endodontics, Kanagawa Dental College, Yokosuka 238-8580, Japan

Periodontal ligament-associated protein-1 (PLAP-1)/asporin is a recently identified novel member of the small leucine-rich repeat proteoglycan family. PLAP-1/asporin is involved in chondrogenesis, and its involvement in the pathogenesis of osteoarthritis has been suggested. We report that *PLAP-1/asporin* is also expressed specifically and predominantly in the periodontal ligament (PDL) and that it negatively regulates the mineralization of PDL cells. *In situ* hybridization analysis revealed that *PLAP-1/asporin* was expressed specifically not only in the PDL of an erupted tooth but also in the dental follicle, which is the progenitor tissue of the PDL during tooth development. Overexpression of PLAP-1/asporin in mouse PDL-derived clone cells interfered with both naturally and bone morphogenetic protein 2 (BMP-2)-induced mineralization of the PDL cells. On the other hand, knockdown of *PLAP-1/asporin* transcript levels by RNA interference enhanced BMP-2-induced differentiation of PDL cells. Furthermore co-immunoprecipitation assays showed a direct interaction between PLAP-1/asporin and BMP-2 *in vitro*, and immunohistochemistry staining revealed the co-localization of PLAP-1/asporin and BMP-2 at the cellular level. These results suggest that PLAP-1/asporin plays a specific role(s) in the periodontal ligament as a negative regulator of cytodifferentiation and mineralization probably by regulating BMP-2 activity to prevent the periodontal ligament from developing non-physiological mineralization such as ankylosis.

Periodontal ligament (PDL)[2] tissue is a connective tissue that is interposed between the roots of the teeth and the inner wall of the tooth-supporting bone (alveolar bone) socket. The collagenous fibers form a meshwork that stretches out between the cementum covering the root surface and the bone and is firmly anchored by Sharpey fibers. The periodontal ligament links the teeth to the alveolar bone proper, providing support, protection, and sensory input to the masticatory system (1). In addition, the PDL also contributes to tooth nutrition, homeostasis, and the repair of damaged periodontal tissue. PDL cells originate in part from the ectomesenchyme of the investing layer of the dental follicle; this developmental origin gives these cells differential properties. Recently it has been revealed that PDL tissue possesses multipotential mesenchymal stem cells that can differentiate into mineralized tissue-forming cells such as osteoblasts and cementoblasts (2, 3). In fact, *in vitro* maintained PDL cells have various osteoblast-like properties, including the capacity to form mineralized nodules, expression of bone-associated markers, and response to bone-inductive factors such as bone morphogenetic protein 2 (BMP-2) (4, 5). Interestingly, however, PDL tissue is never ossified *in vivo* under normal circumstances. This suggests that some mechanisms exist to constitutively prevent unorchestrated osteogenesis and cementogenesis by PDL cells.

Previously we have reported the gene expression profile, described the quantitative aspects of the genes active in the human PDL, and identified a novel gene, *PLAP-1*, that is frequently expressed in human PDL tissue (6). An identical gene has been reported by other groups and named *asporin* because of its unique aspartic acid repeat at the N terminus of the mature protein (7, 8). The *PLAP-1/asporin* gene encodes a novel small leucine-rich repeat proteoglycan (SLRP) protein that resembles decorin and biglycan. Interestingly the expression of the *PLAP-1/asporin* gene was shown to be enhanced during the course of PDL cell cytodifferentiation into mineralized tissue-forming cells and is tightly regulated by BMP-2 (9).

Furthermore a recent report demonstrated that there is a significant association between a polymorphism in the aspartic acid repeat of the gene encoding PLAP-1/asporin and osteoarthritis, which is characterized by the progressive

* This work was supported by Grants-in-aid 17390560 and 17390561 from the Japan Society for the Promotion of Science and was a part of the 21st Century Center of Excellence entitled "Origination of Frontier BioDentistry" at Osaka University Graduate School of Dentistry supported by the Ministry of Education, Culture, Sports, Science and Technology. The costs of publication of this article were defrayed in part by the payment of page charges. This article must therefore be hereby marked "*advertisement*" in accordance with 18 U.S.C. Section 1734 solely to indicate this fact.

[S] The on-line version of this article (available at http://www.jbc.org) contains supplemental Table 1.

[1] To whom correspondence should be addressed: Dept. of Periodontology, Osaka University Graduate School of Dentistry, 1-8 Yamadaoka, Suita, Osaka 565-0871, Japan. Tel.: 81-6-6879-2930; Fax: 81-6-6879-2934; E-mail: ipshinya@dent.osaka-u.ac.jp.

[2] The abbreviations used are: PDL, periodontal ligament; PLAP-1, periodontal ligament-associated protein-1; SLRP, small leucine-rich repeat proteoglycan; BMP, bone morphogenetic protein; TGF, transforming growth factor; RT, reverse transcription; MEM, minimum Eagle's medium; FCS, fetal calf serum; FGF, fibroblast growth factor; ALPase, alkaline phosphatase; shRNA, small hairpin RNA; PBS, phosphate-buffered saline; E, embryonic day; MPDL, murine periodontal ligament; LRR, leucine-rich repeat.

loss of articular cartilage (10–12). It has also been shown that PLAP-1/asporin functioned as a negative regulator of chondrogenesis *in vitro* by inhibiting TGF-β function (10). Both articular cartilage and the PDL are rich in extracellular matrix and have a similar characteristic function, which involves cushioning the mechanical forces of the joints and teeth, respectively. These results suggest the possible involvement of PLAP-1/asporin in the regulation of PDL differentiation into hard tissue-forming cells.

To gain insight into PLAP-1/asporin functions in the PDL, we first examined the tissue distribution of *PLAP-1/asporin in vivo*. *In situ* hybridization analysis demonstrated specific and dominant expression of *PLAP-1/asporin* mRNA in the PDL. Furthermore during tooth development, strong mRNA expression of *PLAP-1/asporin* was observed in the dental follicle, which is the progenitor tissue that forms cementum, alveolar bone, and the PDL. We then examined an *in vitro* model of PDL differentiation that uses a PDL cell clone derived from mouse PDL tissues. Interestingly overexpression of PLAP-1/asporin in PDL cells repressed PDL differentiation and mineralization probably through BMP-2 signaling pathways. Conversely small interference RNA knockdown of *PLAP-1/asporin* in PDL cells augmented PDL differentiation induced by BMP-2. Furthermore co-immunoprecipitation experiments revealed that PLAP-1/asporin could bind to BMP-2 *in vitro*, and two-color immunohistochemistry staining showed co-localization of PLAP-1/asporin and BMP-2 at the cellular level. These data showed that *PLAP-1/asporin* is a periodontal ligament-specific gene that negatively regulates PDL differentiation and mineralization to ensure that the periodontal ligament is not ossified and to maintain homeostasis of the tooth-supporting system.

MATERIALS AND METHODS

RT-PCR Analysis—Total RNA was isolated from mouse tissues and cells using the QIA RNA isolation kit (Qiagen, Santa Clarita, CA) and then purified using the RNAeasy kit (Qiagen). Purified total RNA was reverse transcribed with SuperScript II reverse transcriptase (Invitrogen) with oligo(dT) primer. All PCRs were carried out using AmpliTaq Gold DNA polymerase (Roche Applied Science). The primers used in this study are listed in supplemental Table 1.

Probe Preparation—We subcloned the 709-bp 5′-end/EcoRI fragment, including the 5′-untranslated region and a portion of the open reading frame of mouse *PLAP-1/asporin* gene, into the pGEM-T easy vector (Promega, Madison, WI). The plasmid containing the *PLAP-1/asporin* insert was linearized by digestion with NcoI and SalI restriction enzymes to generate antisense and sense strands, respectively. In the presence of digoxigenin-labeled 11-dUTP (Roche Applied Science), the antisense and sense cRNA probes were prepared by *in vitro* transcription using SP6 and T7 RNA polymerases, respectively.

Northern Blot Analysis—Total RNA (15 μg) isolated from the maxillary and tibial tissues of 4-week-old BALB/c mice was electrophoresed on a 1% formaldehyde-agarose gel and transferred to a nitrocellulose filter (Roche Applied Science). The membranes were then hybridized overnight at 68 °C with digoxigenin-dUTP-labeled antisense single-stranded RNA probes specific for *PLAP-1/asporin* as described above. The blot was washed under high stringency (2× SSC, 0.1% SDS at room temperature) and low stringency (0.1× SSC, 0.1% SDS at 68 °C) conditions. The reaction was then blocked using the DIG (digoxigenin) Wash and Block Buffer Set (Roche Applied Science) according to the manufacturer's protocol. The hybrids were detected using the anti-digoxigenin-alkaline phosphatase Fab fragment (Roche Applied Science).

Tissue Preparation and in Situ Hybridization—To analyze erupted teeth, 4-week-old BALB/c mice were anesthetized by intraperitoneal injection of Nembutal (50 mg/kg of body weight) and intracardially perfused with physiological saline containing 5 units/ml heparin (Aventis Pharma, Tokyo, Japan) for 2–3 min followed by perfusion with 5% paraformaldehyde in 0.1 M sodium phosphate buffer (pH 7.4) at 4 °C for 15 min. The upper jaw samples containing the teeth were excised, and most of the soft tissue was removed. All of the samples were further fixed by immersion in the fixative described above overnight at 4 °C and then demineralized in buffered 10% EDTA at 4 °C under agitation for 7 days. The EDTA solution was changed daily. After processing, the blocks were rinsed and embedded in paraffin. Serial 5-μm-thick sections were cut in the transverse direction for the first molars and mounted onto aminopropylsilane-coated slides. Representative sections from each block were stained with hematoxylin and eosin. *In situ* hybridization of developing tooth germ was carried out on the fresh frozen horizontal sections of BALB/c mice fetal heads. The sections were fixed in 4% paraformaldehyde for 10 min, and this was followed by acetylation.

In situ hybridization was performed as described previously (13). We used the cRNA probe of *PLAP-1/asporin* described above. The sections were deparaffinized in xylene, hydrated, postfixed in 4% paraformaldehyde, and sequentially treated with 10 mg/ml proteinase K at 37 °C for 30 min and with 0.1 M triethanolamine containing 0.25% acetic anhydride for 10 min. Hybridization was done at 50 °C under high stringency conditions using the denatured probes at concentrations of about 1 ng/ml in a freshly prepared hybridization mixture. All samples were hybridized overnight at 50 °C. Posthybridization treatment included incubation with RNase A at 37 °C for 30 min followed by thorough washes. The washed slides were incubated with anti-digoxigenin monoclonal antibody (Roche Applied Science) overnight at 4 °C. After the application of biotinylated rabbit anti-mouse IgG antibody (Dako, Glostrup, Denmark), the sections were incubated with alkaline phosphatase-conjugated streptavidin (Dako) and then with nitro blue tetrazolium/5-bromo-4-chloro-3-indolyl phosphate solution (Roche Applied Science) for 3–5 h to visualize the hybridized sites. The activity of endogenous bone alkaline phosphatases in these specimens was inhibited by heating during paraffin embedding at 60 °C for 6 h. Negative controls for *in situ* hybridization were obtained by substituting the antisense probe with its sense probe.

Cloning of Mouse PDL Cell Line—Mouse PDL cells were obtained from the PDL tissues of the molar teeth obtained from 2.5-week-old BALB/c mice. The PDL tissues were scraped from the middle of one-third of the root surface and transferred into 24-well plates. The outgrown cells from the explants were cultured in α-MEM supplemented with 10% FCS, 10 ng/ml FGF-2 (Kaken, Kyoto, Japan), and 60 μg/ml kanamycin (Meijiseika, Tokyo, Japan). The cultures were maintained at 37 °C in a humidified atmosphere of 95% air and 5% CO_2. At subconfluence, the cells were passaged with trypsin-EDTA and cultured on tissue culture plates. After 12 subcultures, the cell suspension was diluted and plated on 96-well plates at a ratio of one or two cells per well. Cell cloning was done twice using the limiting dilution method in α-MEM supplemented with 10% FCS and 100 ng/ml FGF-2. Twenty-nine clonal cell lines were obtained and classified by alkaline phosphatase (ALPase) activity. One clonal cell line possessing the highest ALPase activity was selected and named MPDL22. The preosteoblastic cell line MC3T3-E1 was a generous gift from Prof. Toshiyuki Yoneda (Osaka University, Osaka, Japan).

Plasmids—We cloned the open reading frame of mouse *PLAP-1/asporin* gene into pCI-neo (Promega). We confirmed whole sequences of the insert by DNA sequencing and named it pCI-neo-PLAP-1/asporin. We used the pCI-neo plasmid vector without the insert as a negative control. We also cloned the open reading frame of mouse *PLAP-1/asporin* into p3XFLAG-CMV-14 (Sigma) in which the 3XFLAG protein can be fused to the C terminus of the insert. We named it p3XFLAG-PLAP-1/asporin. We used the p3XFLAG-CMV-14 vector without the insert as a negative control.

Cell Culture and Transfection—We maintained the MPDL22 cells in a standard medium of α-MEM supplemented with both 10% FCS and 100 ng/ml FGF-2. For stable transfections, we plated 5×10^4 of the MPDL22 cells/well in a 6-well plate. After 12 h, we transfected the cells with the pCI-neo-PLAP-1/asporin expression vector or the p3XFLAG-PLAP-1/asporin expression vector using Effectene transfection reagent (Invitrogen) in accordance with the manufacturer's protocol. After 24 h, we added G418 (400 μg/ml) to the culture medium to initiate drug selection. After selection, we evaluated *PLAP-1/asporin* expression using RT-PCR. We then established the stable transfectants overexpressing PLAP-1/asporin.

To differentiate transfected MPDL22 cells into hard tissue-forming cells *in vitro*, we cultured cells in a 24-well plate until they reached confluence. At this point, we removed FGF-2 from the culture medium and replaced the standard medium with α-MEM supplemented with 10% FCS, 10 mM β-glycerophosphate, and 50 μg/ml ascorbic acid (mineralization medium). We replaced the mineralization medium every 3 days. During the culture of the transfectant cells, we always added 400 μg/ml G418 to the mineralization medium.

To examine the effects of PLAP-1/asporin on BMP-2-induced cytodifferentiation, transfectant cells were cultured in standard medium in a 24-well plate until they reached confluence. On the next day, the medium was replaced with FCS-free α-MEM. After serum deprivation for 24 h, the cells were stimulated with 100 ng/ml BMP-2 (R&D Systems, Minneapolis, MN) in FCS-free α-MEM. The stimulated cells were then harvested at 24, 48, and 72 h after stimulation to assess ALPase activity.

RNA Interference of PLAP-1/Asporin—The small interference RNA oligonucleotide against mouse *PLAP-1/asporin* was designed according to Reynolds *et al.* (14). The target sequences included 5′-CGA TGA TGA CGA CAA CTC T-3′ and 5′-CCT GCA ACA TTT CGT TGT G-3′, which are located at nucleotides 326–344 and 1260–1278 of the mouse *PLAP-1/asporin* gene (GenBank™ accession number NM_025711), respectively. The pSilencer RNA interference kit (Ambion, Austin, TX) was used for generating small hairpin RNA (shRNA). We used a negative control shRNA oligonucleotide from the Ambion kit that is unrelated to *PLAP-1/asporin*. Briefly a double-stranded DNA oligonucleotide containing the shRNA and BamHI and HindIII overhangs was cloned into the BamHI and HindIII sites of the pSilencer 2.1-U6 hygro vector (Ambion), an expression vector designed to express shRNAs using the U6 promoter. The constructs were verified by DNA sequencing. The shRNA vectors were introduced into MPDL22 cells by Nucleofection (Amaxa, Gaithersburg, MD) according to the manufacturer's protocol. We started drug selection by hygromycin (600 μg/ml) 24 h after transfection.

Alkaline Phosphatase Activity and Mineralization Assay—ALPase activity was assessed according to the procedure of Bessey *et al.* (15). Briefly after washing twice with PBS, the cells were homogenized in a glass homogenizer in 1 ml of 0.9% NaCl, 0.2% Triton X-100 at 4 °C and then centrifuged for 15 min at 12,000 × *g*. ALPase activity in the supernatant was measured using *p*-nitrophenyl phosphate as a substrate. Subsequently the supernatant was mixed with 0.5 M Tris-HCl buffer (pH 9.0) containing 0.5 mM *p*-nitrophenyl phosphate and 0.5 mM $MgCl_2$. Next the samples were incubated at 37 °C for 30 min, and the reaction was stopped by addition of 0.25 ml of 1 N NaOH. Using a spectrometer, hydrolysis of *p*-nitrophenyl phosphate was monitored as a change in A_{410}; *p*-nitrophenol was used as a standard. One unit of activity was defined as the enzyme activity hydrolyzing 1 nmol of *p*-nitrophenyl phosphate in 30 min. The histochemical method that was used for staining calcified nodules was done using the alizarin red staining method of Dahl (16). The cell layers were washed twice with PBS and then fixed in dehydrated ethanol. After fixation, the cell layers were stained with 1% alizarin red S in 0.1% NH_4OH (pH 6.3–6.5) for 5 min. The dishes were washed with H_2O and then observed microscopically.

Cellular DNA Contents—DNA content was measured using a modification of the method of Labarca and Paigen (17). The cells were washed with PBS and then homogenized at 4 °C in 1 ml of 2 M NaCl, 25 mM Tris-HCl (pH 7.4). After centrifugation at 12, 000 × *g* for 10 min, 25 μl of 5 μg/ml bisbenzimidazole (Hoechst 33258) were added to 100 μl of the supernatant. After excitation at 356 nm, the fluorescent spectra of the emission at 458 nm were monitored using a spectrophotometer (microplate reader MTP-32, Corona Electric, Ibaragi, Japan). The concentration of DNA in the samples was determined using a standard curve based on various concentrations of calf thymus DNA.

[³H]Thymidine Incorporation Assay—The proliferation activity of the *PLAP-1/asporin* overexpressing transfectant cells and *PLAP-1/asporin* shRNA transfectant cells was assessed by measuring the [³H]thymidine incorporation. The cells were seeded to 24-well culture dishes (1×10^4 cells/well). On the next day, the medium was replaced with FCS-free α-MEM. After serum deprivation for 24 h, the cells were stimulated with α-MEM containing 10% FCS for 24 h. DNA synthesis was measured by pulsing wells with 2 μCi/well [³H]thymidine for 4 h. The cells were then washed three times with PBS, and soluble radioactivity was extracted with 5% trichloroacetic acid. The cells were solubilized in 1 N NaOH, and lysate was brought to a neutral pH by addition of 6 N HCl. The incorporated radioactivity was determined in a liquid scintillation counter (Aloka, Tokyo, Japan) using an aqueous scintillation mixture.

Expression and Purification of Recombinant PLAP-1/Asporin—Recombinant mouse PLAP-1/asporin protein was generated from baculovirus-infected silkworms as described previously (18). Briefly we subcloned the full length of mouse *PLAP-1/asporin* cDNA into the transfer vector pSYNGCH_Th that was to be fused to a His tag in the C terminus. Then the plasmid was co-transfected with the linearized baculovirus DNA BacDuo (Katakura Industries, Saitama, Japan) into the *Spodoptera frugipedra* cell line SF21AE. Three days after transfection, the culture supernatants containing the recombinant baculovirus were harvested. The recombinant virus was injected into the body cavities of silkworm larvae (8.0×10^5 plaque-forming units/head). The whole body of the infected larvae was mechanically blended in lysis buffer (20 mM Na_2PO_4, pH 7.5, 10% glycerol, 0.15 M NaCl, 1 mM phenylmethylsulfonyl fluoride, 10 mM benzamide, 1 mM dithiothreitol, 1 mM EGTA, 1 mM EDTA). Homogenized lysates were centrifuged at $80,000 \times g$ for 60 min, and the supernatants were then diluted five times by dilution buffer (20 mM NaH_2PO_4, pH 8.0, 0.3% Zwittergent 3-14). The diluted solution was loaded on a nickel-Sepharose column. After washing with washing buffer (20 mM NaH_2PO_4, pH 8.0, 0.3% Zwittergent 3-14), His-tagged mouse PLAP-1/asporin was eluted by elution buffer (20 mM Tris-HCl, pH 8.0, 0.3 M NaCl, 250 mM imidazole, 10% glycerol, 0.1% Zwittergent 3-14, 0.05% 2-mercaptoethanol).

To confirm the quality of recombinant protein, the elution sample was subjected to SDS-PAGE (5–20% gradient gel). The proteins separated in the gel were stained using Silver Stain II kit (Wako, Osaka, Japan). After the SDS-PAGE, electroblotting onto polyvinylidene difluoride membranes was performed. The membranes were incubated in TBST (50 mM Tris-HCl, pH 7.5, 150 mM NaCl, 0.1% (v/v) Tween 20) with 5% (w/v) nonfat dried milk at 4 °C overnight, washed in TBST three times, and incubated with primary antibody in TBST containing 5% milk for 1 h at room temperature. The primary antibody was a rabbit polyclonal anti-polyhistidine antibody (Santa Cruz Biotechnology, Santa Cruz, CA) at 1:1,000. After further washing in TBST, membranes were incubated for 1 h with horseradish peroxidase-linked anti-rabbit IgG secondary antibody (Amersham Biosciences), and immunoreactive proteins were detected using the ECL kit (Amersham Biosciences).

Co-immunoprecipitation Assay and Western Blotting—Recombinant PLAP-1/asporin protein (1.2 μg) was incubated with 3.0 μg of BMP-2 for 1 h at 4 °C in 0.5 ml of binding buffer (50 mM Tris-HCl, pH 7.5, 150 mM NaCl, 1% Triton X-100, Complete protease inhibitor mixture (Roche Applied Science)). Then 7.5 μl of anti-polyhistidine antibody-conjugated agarose (Santa Cruz Biotechnology) or 40 μl of anti-BMP-2 antibody (Calbiochem-Novabiochem)-conjugated Protein G-Sepharose (Amersham Biosciences) were added to the reaction and incubated for 1 h at 4 °C. The precipitates were washed three times with binding buffer, subjected to 15% SDS-PAGE, and then electroblotted onto polyvinylidene difluoride membranes. The membranes were incubated in TBST with 5% (w/v) nonfat dried milk at 4 °C overnight, washed in TBST three times, and incubated with primary antibody in TBST containing 5% milk for 1 h at room temperature. The primary antibodies were a rabbit polyclonal anti-polyhistidine antibody at 1:1,000 and a goat polyclonal anti-BMP-2/4 antibody (R&D Systems) at 1:250. After further washing in TBST, membranes were incubated for 1 h with horseradish peroxidase-linked anti-rabbit IgG secondary antibody (Amersham Biosciences) or anti-goat IgG secondary antibody (Santa Cruz Biotechnology), and immunoreactive proteins were detected using the ECL kit.

Immunohistochemistry—The FLAG-tagged PLAP-1/asporin-transfected MPDL22 cells were seeded on a collagen type I-coated 10-mm glass-bottomed dish (Matsunami, Osaka, Japan). On the next day, to detect BMP-2 binding, the cells were preincubated with BMP-2 (10 μg/ml) for 2 h at 37 °C and washed with PBS three times. The cells were fixed in a mixture of methanol:acetone (1:1) for 1 min at room temperature, then washed with PBS three times, and preblocked in PBS containing 10% bovine serum albumin (Sigma) for 30 min at room temperature. The BMP-2-positive cells were identified by incubation with biotinylated anti-BMP-2/4 antibody (2.5 μg/ml, R&D Systems) overnight at 4 °C and subsequently streptavidin-rhodamine red (Invitrogen) for 1 h at room temperature. After washing with PBS, the cells were incubated with fluorescein isothiocyanate-conjugated anti-FLAG antibody (Sigma) for 1 h at room temperature. Then the cells were washed, and the nuclei were stained with 4′,6-diamidino-2-phenylindole (Vector Laboratories, Burlingame, CA).

Statistical Analysis—All of the experiments in this study were conducted at least three times. The data shown are representative results. Experimental values are given as means ± S.D. of triplicate assays. The statistical significance of the differences between two means was examined by the Mann-Whitney *U* test; *p* values less than 0.05 were considered to indicate a significant difference.

RESULTS

Specific Expression of PLAP-1/Asporin in the Periodontal Ligament—We analyzed *PLAP-1/asporin* expression in various mouse tissues. RT-PCR analysis revealed dominant expression of *PLAP-1/asporin* in the maxilla, which contains teeth and periodontal tissues consisting of gingiva, cementum, alveolar bone, and the PDL (Fig. 1*A*). Our previous study showed dom-

inant expression of *PLAP-1/asporin* in human PDL tissue (6). On the other hand, *PLAP-1/asporin* mRNA has been shown to be expressed abundantly in the heart in both mice and humans (7, 8). However, as Fig. 1*A* indicates, the maxilla, which contains PDL tissues, had a higher expression of *PLAP-1/asporin* mRNA than the heart (Fig. 1*A*). These results prompted us to investigate the specific expression of *PLAP-1/asporin* in periodontal tissues.

Next we performed Northern blot analysis to assess the *in vivo* expression of *PLAP-1/asporin* mRNA in the maxilla, which includes both teeth and periodontal tissues. We selected the 5′-region of *PLAP-1/asporin* mRNA, which has nucleotide sequences specific to *PLAP-1/asporin*, to use as a probe. The analysis revealed specific detection of the 2.3-kb transcript of *PLAP-1/asporin* in the maxilla (Fig. 1*B*). Notably there was no *PLAP-1/asporin* signal in the bone tissue obtained from the tibia, suggesting that *PLAP-1/asporin* is not expressed in the bone compartment of the maxilla.

We then carried out an *in situ* hybridization analysis of *PLAP-1/asporin* expression in mouse maxilla specimens. *PLAP-1/asporin* was expressed only in PDL tissue (Fig. 2*A*).

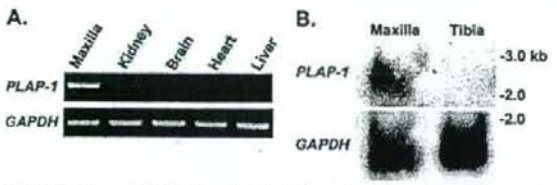

FIGURE 1. **Tissue distribution of *PLAP-1/asporin* mRNA.** *A*, RT-PCR analysis in various tissues from 4-week-old BALB/c mice. The number of PCR cycles was 28 and 22 for *PLAP-1/asporin* and glyceraldehyde-3-phosphate dehydrogenase (*GAPDH*), respectively. *B*, Northern blot analysis in the maxilla and tibia. Total RNA (15 μg) from the maxilla and tibia was electrophoresed.

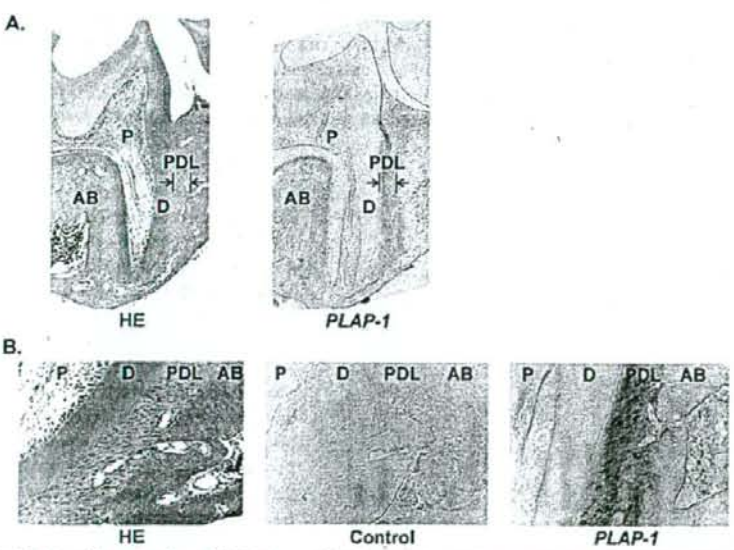

FIGURE 2. **Specific expression of *PLAP-1/asporin* in the periodontal ligament *in vivo*.** *A*, *in situ* hybridization analysis in the mouse maxilla from 4-week-old BALB/c mice. *B*, higher magnification. *HE*, hematoxylin and eosin stain; *PLAP-1*, antisense probe for *PLAP-1/asporin*; *Control*, sense probe for *PLAP-1/asporin*; *P*, pulp; *D*, dentin; *AB*, alveolar bone. *Original magnification*, ×50 in *A* and ×200 in *B*.

High magnification showed broad and intense expression of *PLAP-1/asporin* mRNA in the PDL tissue (Fig. 2*B*). No expression was observed in alveolar bone or other periodontal tissues such as gingival tissue, the bone marrow of alveolar bone, or dental pulp tissue. This suggests that PLAP-1/asporin presumably plays a particular *in vivo* role in the periodontal ligament tissue.

PLAP-1/Asporin Expression during Tooth Development—To obtain a more complete picture of *in vivo PLAP-1/asporin* expression in the periodontal ligament, particularly during tooth development, we performed an *in situ* hybridization analysis of tooth germs at different stages of development. As shown in Fig. 3*A*, around embryonic day 13 (E13), the dental epithelium invaginates into the neural crest-derived dental ectomesenchyme and forms the epithelial bud, which is known as the bud stage. Subsequently during the following cap stage around E15.5, the dental epithelium starts to differentiate into inner and outer dental epithelia. During the early bell stage around E18, specific cusp pattern formation commences. During the late bell stage, which occurs around postnatal day 1, dentin matrix is secreted at the tip of the cusps by functional odontoblasts, and terminal differentiation of ameloblasts begins.

No expression of *PLAP-1/asporin* mRNA was observed in the tooth germ at the bud stage at E13 (Fig. 3*B*). Then at the cap stage, strong expression was detected only in the dental follicle, which originates from the neural crest-derived ectomesenchyme (Fig. 3*C*). The dental follicle gives rise to the periodontal tissues consisting of periodontal ligament, cementum, and alveolar bone. *PLAP-1/asporin* mRNA was expressed neither in the dental papilla, which forms the dentin and pulp, nor in the dental epithelium. During the bell stage, continuous expression of *PLAP-1/asporin* was observed in dental follicles, especially in those in which tooth root formation was taking place (Fig. 3, *D* and *E*). Taken together, the data indicate that *PLAP-1/asporin* is initially expressed in the dental follicle cells during tooth germ development, and specific expression of *PLAP-1/asporin* becomes progressively evident in adult PDL tissue.

Establishment of the Mouse Periodontal Ligament Cell Line MPDL22—To analyze PLAP-1/asporin function *in vitro*, we established PDL cell clones from mouse PDL tissue. Utilizing the dilution cloning method in the presence of FGF-2, we obtained 29 cell clones from explant cultures of mouse PDL tissue. To assess their ability for cytodifferentiation into hard tissue-forming cells, we cultured each cell clone in the mineralization medium for 8 days (Fig. 4).